



**CHALMERS**

---

# CPL

*Chalmers Publication Library*

Institutional Repository of  
Chalmers University of Technology  
<http://publications.lib.chalmers.se>

---

This is the pre-peer reviewed version of the following article:

**Pischel, U. et al.**  
**Information Processing with Molecules - Quo Vadis?**  
**ChemPhysChem, 2013, Vol.14, Issue 1, pp 28-46**

The article has been published in final form at:

<http://dx.doi.org/10.1002/cphc.201200157>

Access to the published version may require subscription.  
Published with permission from:

**Wiley**

## Information Processing with Molecules – *Quo Vadis?*

Uwe Pischel,<sup>\*[a]</sup> Joakim Andréasson,<sup>\*[b]</sup> Devens Gust,<sup>[c]</sup> Vânia F. Pais<sup>[a]</sup>

<sup>[a]</sup> Center for Research in Sustainable Chemistry and Department of Chemical Engineering, Physical Chemistry, and Organic Chemistry, University of Huelva, Campus de El Carmen s/n, E-21071 Huelva, Spain

Email: uwe.pischel@diq.uhu.es; Fax : (+34) 959 21 99 83

<sup>[b]</sup> Department of Chemical and Biological Engineering, Physical Chemistry, Chalmers University of Technology, SE-412 96 Göteborg, Sweden

Email: a-son@chalmers.se; Fax: (+46) 31 772 38 58

<sup>[c]</sup> Department of Chemistry and Biochemistry, Arizona State University, Tempe, Arizona 85287-1604, United States

**Lead-In.** Information processing at the molecular level is coming of age. Since the first molecular AND gate was proposed *ca.* 20 years ago, the molecular interpretation of binary logic has become vastly more sophisticated and complex. However, the field is also at a crossroads. While cleverly designed molecular building blocks are abundant, difficult questions remain. How can molecular components be flexibly assembled into larger circuits, and how can these components communicate with one another. The concept of all-photonic switching with photochromic supermolecules has shown some interesting potential and is discussed in this Review. Although the field of molecular logic was originally discussed mainly in terms of a technology that might compete with solid-state computers, potential applications have expanded to include clever molecular systems and materials for drug delivery, sensing, probing, encoding, and diagnostics. These upcoming trends, which are herein illustrated by selected examples, deserve general attention.

**Keywords.**

Molecular devices • drug delivery • materials science • photochromism • fluorescence

## Introduction

Ones and zeros – the universal digital language used by microprocessors – has been adopted for almost 20 years to describe the physicochemical properties of molecules using Boolean algebra, also known as switching algebra. The chemical bi-stability of many molecular systems makes them *per se* excellent candidates to represent events/properties in terms of 1 or 0 by switching the molecule between the two states using external stimuli. Although molecular switching (e.g. using acid/base chemistry) has been known for a long time, it was not until the demonstration of the molecular AND gate (**1**; see structure in Scheme 1) by de Silva and co-workers in 1993 that the behavior was interpreted in terms of Boolean logic.<sup>[1]</sup> Since then, all existing 2-input logic gates have been realized on the molecular scale, as have a large variety of more complex devices<sup>[2-11]</sup> such as adders and subtractors,<sup>[9, 12, 13]</sup> multiplexers/demultiplexers,<sup>[14-17]</sup> encoders/decoders,<sup>[18, 19]</sup> keypad locks,<sup>[20-26]</sup> latches/flip-flops,<sup>[10, 27-34]</sup> and multivalued logic devices.<sup>[35, 36]</sup> The initial impetus for conducting research in molecular logic has been to make molecules imitate the functions of silicon circuitry, the main objectives being miniaturization (*via* a bottom-up approach) and implications thereof, such as minimal power consumption. Although elegant proof-of-principle studies indeed show that cleverly designed molecules are able to process the information contained in the input signals and deliver output responses according to the function of the respective logic device, there are several barriers to overcome before molecular devices can compete with their silicon-based big brothers. First, the majority of the abovementioned studies have been performed in fluid solution using concentrations in the micromolar range. Although “wet” computers could have applications in alternative milieus, they would be of very limited use as substitutes for the conventional personal computer. That is why the transfer of molecular logic

principles to solid state materials is a foremost task. It is also desirable to perform the logic operations on the single molecule scale, or at least using small ensembles of molecules. Second, increased functional complexity in conventional circuitry is achieved by physically integrating several logic gates through wiring (concatenation) in combinational and sequential circuits. This approach is not easily applied using molecules as the individual logic gates, often due to input/output inhomogeneity (the physical nature of the output of an upstream gate is not the same as the input of the downstream gate). All-photonic systems, which rely on optical inputs and outputs, formally overcome this barrier. The multidirectional nature of light emitted by a molecule, however, makes the direct feeding of emission-based photonic output into the input of another gate a non-trivial task. Only a few proof-of-principle examples of concatenated chemical systems have been reported in the literature.<sup>[8, 37-45]</sup>

During the last 5 years it has become evident that molecular information processing is not restricted to the mimicry of the functions performed by silicon-based electronic devices. Fields where semiconductor materials cannot go will likely lead to practical applications before molecular computers become a reality. Biological systems, e.g., the human body, are identified in this context. To mention a few applications, molecules with logic functionality can be applied as multi-parameter sensors for diagnostic purposes or as interfaces for pro-drug activation. Furthermore, there are several examples where molecular logic has been used in the development of intelligent materials such as nanovalves and polymers. These latest developments of molecular logic along such lines will be documented and discussed in later sections of this Review.

Initially, however, we will discuss the use of molecules to mimic some of the functions of silicon-based logic devices, and will introduce two important concepts

which are difficult to realize in silicon devices but readily achievable in the world of molecular logic: *functional integration* and *reconfiguration*. The former is being used to overcome the need for concatenation, and the latter is a property of molecular logic devices which vastly increases their flexibility and utility.

### **Advanced logic operations through functional integration and reconfiguration**

In Scheme 2 the logic diagram for the 4-2 encoder is shown. This device translates numbers in base 10 to base 2 (binary numbers). The device consists of an AND gate, an OR gate, and two NOT gates, physically integrated through hardwiring. One approach to mimic the function of the 4-2 encoder on the molecular scale would be to design one molecular AND gate, another molecular OR gate, and finally two molecular NOT gates. These gates would then have to be concatenated according to the logic scheme in order to direct the output signals from the upstream gates to the downstream gates. A frequently used approach for molecular logic gates (*vide infra*) is that the inputs are represented by the addition of chemical species whereas the outputs are read as optically detectable signals, e.g., absorbance or intensity of emission. Let us discuss a hypothetical example: if the outputs from the NOT gates (triangles) in Scheme 2 would be read as the intensity of emission of light from some chromophore at a certain wavelength, and the inputs of the AND gate (which ultimately delivers output Out1) are two distinct cations it is easily realized that it is impossible to directly feed the output signals from the NOT gates to the inputs of the AND gate due to their different physical nature. This situation is referred to as input/output inhomogeneity. As mentioned above, all-photonics molecular gates/devices formally overcome this problem. However, if, as above, a gate output is the emission (fluorescence or phosphorescence) from a chromophore, this light is typically emitted in all directions, rather than as a discrete

beam directed to the AND gate. This multidirectional nature of emitted light makes concatenation difficult even for these systems.

An alternative to physical integration is *functional* integration, where the function of a complex logic circuit, such as the 4-2 encoder, is designed into one (supra)molecular species, rather than implemented with separate molecules representing each logic gate in the circuit. Molecular logic devices which correspond to functionally integrated circuits with up to 20 logic gates have been demonstrated.<sup>[46]</sup> A simpler case of functional integration, but one of the pioneering examples, was reported by de Silva and McClenhagan in 2002 where a “receptor<sub>1</sub>-ICT chromophore-receptor<sub>2</sub>” system (**2**; see Scheme 1) was used as the molecular platform.<sup>[47]</sup> It was found that acid could be used together with Ba<sup>2+</sup> or Sr<sup>2+</sup> ions to mimic the function of an exclusive OR (XOR) gate by monitoring the transmittance of a solution at 402 nm. The Ba<sup>2+</sup> and Sr<sup>2+</sup> ions induced the same type of chemical/spectroscopic changes, so that this scheme can be interpreted as Ba<sup>2+</sup> and Sr<sup>2+</sup> serving as the input to an OR gate, where the corresponding output functions as the input to an XOR gate together with H<sup>+</sup> as the second input.

Although the abovementioned example indeed integrated OR and XOR logic, the circuit did not perform any essential arithmetic/logic operation. The addition and subtraction of binary numbers definitely qualify as essential, and in 2000 the de Silva group published the first molecular half-adder based on a “cocktail” (mixture in solution) of two molecular logic gates (XOR and AND).<sup>[48]</sup> In 2003 and 2004 the first experimental realizations of a *unimolecular* half-adder (HA) and a half-subtractor (HS) were reported by the groups of Zhu/Zhang and Langford, respectively.<sup>[49-51]</sup> A HA performs the addition of two binary digits, whereas a HS effectuates the corresponding subtraction. With the use of binary numbers, the four operations of the HA are  $0 + 0 =$

00,  $0 + 1 = 01$ ,  $1 + 0 = 01$ , and  $1 + 1 = 10$ , commonly represented by the truth table of the HA as shown in Table 1.

**Table 1.** Truth table of a half adder.

In1	In2	Out1 AND (C)	Out2 XOR (S)	Binary Sum	10-base sum
0	0	0	0	00	0
0	1	0	1	01	1
1	0	0	1	01	1
1	1	1	0	10	2

Here, it is seen that the HA consists of two binary inputs (In1 and In2) and two binary outputs (Out1 and Out2). The inputs represent the two binary digits to be added, and the outputs represent the two least significant bits of the binary sum. The output that corresponds to the carry digit (C) is described by an AND gate, whereas the corresponding gate for the sum digit (S) output is described by the XOR gate. The HS performs subtraction of the two binary digits according to  $0 - 0 = 00$ ,  $1 - 0 = 01$ ,  $0 - 1 = 11$ , and  $1 - 1 = 0$ . Here, the outputs of the borrow (B) and the difference (D) digits are described by inhibit (INH) and XOR logic, respectively.

The unimolecular half-adder **3** (see Scheme 3) reported by Zhu and Zhang was based on a photochromic spiropyran molecule and used UV light and  $\text{Fe}^{3+}$  ions as inputs.<sup>[49]</sup> With the initial state in the spiro (SP) form, which absorbed exclusively in the UV region of the spectrum, UV exposure triggered the isomerization to the merocyanine (MC) form with a concomitant rise of the absorbance of the solution at 520 nm. Alternatively, if  $\text{Fe}^{3+}$  ions were added to the SP form, the absorption at 520 nm grew in as well, due to the oxidation of SP to  $\text{SP}^{\bullet+}$ . If the SP form was instead exposed to UV light and  $\text{Fe}^{3+}$ ,  $\text{MC-Fe}^{3+}$  was generated. This species was the strongest absorber

at 420 nm, whereas the absorbance at 520 nm was practically zero. With a proper choice of threshold levels, these absorbance changes allowed for a straightforward interpretation of the HA by monitoring the absorbance at 420 nm and 520 nm as the outputs for the AND gate and the XOR gate, respectively.

The HS reported by Langford was realized with a tetraphenyl-substituted free base porphyrin (TPPH<sub>2</sub>, **4** in Scheme 1) where acid and base were used as the inputs.<sup>[50, 51]</sup> The Soret band absorption maximum of TPPH<sub>2</sub> was found at 417 nm. Addition of acid or base resulted in the formation of the dication TPPH<sub>4</sub><sup>2+</sup> or the dianion TPP<sup>2-</sup>, respectively. These species showed pronounced changes in the absorption spectra compared to TPPH<sub>2</sub>. Most importantly, the absorption at 417 nm was virtually zero for both the dication and the dianion. Simultaneous addition of acid and base resulted in the preservation of TPPH<sub>2</sub> as the acid and the base neutralized each other, and the absorbance at 417 nm remained high. Monitoring the transmittance at 417 nm for the different input combinations resulted in the XOR gate, as addition of acid or base alone switched the output *on*, whereas their simultaneous addition left the output in the *off* state. The corresponding INH gate was realized by monitoring the emission intensity at 440 nm, which concluded the truth table of the HS. Since these pioneering reports, a large number of molecular HA and HS has been described in the literature, and several of these studies were discussed in comprehensive reviews.<sup>[9, 11]</sup>

Until 2005, separate molecules were used to realize the functions of the HA and the HS, respectively, i.e., there was no report of a molecule capable of performing addition as well as subtraction (the functions of a so-called *moleculator*). Interestingly, the first molecule shown to do so was the well-known fluorescent pH-indicator fluorescein (**5**; see Scheme 1), in a report by Shanzer and co-workers.<sup>[52]</sup> Fluorescein exists in four different protonation states, each possessing distinct UV/vis spectral

features. By the use of acid and base as inputs, the HA was realized by monitoring the absorbance at two different wavelengths, whereas degenerate inputs in form of base were used as inputs for the corresponding HS. A year later, the same group extended the studies on fluorescein and acid/base chemistry to target also the full-adder (FA) and the full-subtractor (FS) functions.<sup>[13]</sup> In conventional electronics, the FA and the FS are constituted by the physical integration of an OR gate and, respectively, two HA and two HS. The arithmetic operations performed by the FA and the FS are the addition and the subtraction of three bits, where each bit is represented by an input. Hence, the FA and the FS operate with three inputs and two outputs. Rather than letting each of the inputs be represented by distinct chemical species, Shanzer and co-workers reduced the set of inputs to acid and base only, and the absorption/transmittance was read at carefully chosen output wavelengths. Switching between the addition and subtraction modes was done by changing the inputs, the initial state, and the readout wavelengths. Hence, one and the same molecular platform can be used to perform two separate logic operations by simple re-definitions of the inputs and the outputs. This is referred to as *reconfiguration* - a property of molecular systems that is not inherently shared by silicon-based circuitry, where the logic operation typically is defined in an unchangeable manner. In a later section we will present an extreme example of input/output reconfiguration, allowing for a molecular triad to perform no less than 13 different logic operations, sharing a common initial state.<sup>[53]</sup>

Another instructive example of the successful application of reconfiguration is the unimolecular multiplexer/demultiplexer reported by Credi and co-workers in 2008.<sup>[14]</sup> A 2:1 multiplexer (MUX) has two data inputs (In1 and In2), one selector input (Sel), and one output (Out). Depending on the state of Sel, the state of either In1 or In2 is directly transmitted to the output Out. Hence, the information contained in two data

lines is combined into one common transmission line. The 1:2 demultiplexer (DEMUX) performs the opposite operation, i.e., it separates the information on the input transmission line In into two separate output lines (Out1 and Out2), depending on the state of the address input (Ad). Typically, In is the same line as the output Out from a MUX. In this way, the information carried by the data lines initially fed into the MUX (In1 and In2) is directed to Out1 and Out2, respectively, *via* a common intermediate transmission line. Credi and co-workers used the 8-methoxy-substituted quinoline derivative **6** (see Scheme 1) as the molecular platform. Upon addition of acid, **6-H<sup>+</sup>** was formed, with concomitant changes in the absorption and the emission spectra. Both forms emitted significantly at 474 nm, whereas **6** and **6-H<sup>+</sup>** were the major light absorbers at 285 nm and 350 nm, respectively. Using acid as Sel, excitation light at 285 nm and 350 nm were defined as the inputs for the MUX, and the emission intensity at 474 nm was used as the corresponding output. A similar approach was followed in the realization of the DEMUX using excitation at the isosbestic point at 262 nm as the input In, acid as Ad input, and emission at 388 nm (emission maxima for **6**) and 500 nm (emission maxima for **6-H<sup>+</sup>**) as the outputs.

In the following section, we describe a photochromic molecular platform which allows functional integration and reconfiguration of 13 logic operations in an all-photonic manner. This multifaceted molecular logic building block focuses all concepts discussed above and constitutes a state-of-the-art example of chemists' imagination marrying electronic and molecular data processing.

### **All-photonic Switching as Idealized Approach Toward Molecular Computers**

A common denominator for all molecular logic devices described above is that chemicals were used as inputs to trigger the chemical transformations in solution, and

the resulting spectral changes were read as outputs. This implies that the reactions are diffusion-controlled, and, hence, less suitable in rigid media. Furthermore, repeated cycling of the operations will lead to the buildup of chemical waste and/or dilution effects, if the chemical transformations are at all reversible to allow for repeated use. This limits the number of repeat operations that a given sample can perform. An alternative approach is to use light as inputs to trigger the corresponding chemical changes and also to read the resulting outputs as optical signals. Devices operated according to this principle are referred to as all-photon devices. As opposed to systems with chemical inputs, the all-photon operation is waste-free and does not require physical access, facilitating remote operation and the use of monolithic structures containing the molecular logic elements.

Furthermore, using photons as inputs and outputs overcomes at least formally the input/output inhomogeneity barrier, which is a prerequisite for direct concatenation of several molecular logic devices. Photochromic molecules, which are reversibly photochemically isomerizable, have been identified as excellent candidates for all-photon logic platforms due to their inherent bistability, allowing for a straightforward 0/1 assignment to the two isomeric forms (or selected properties of the two isomeric forms).<sup>[6, 7]</sup> Combining two or more separate photochromic units into higher molecular architectures (dyads, triads *etc.*) facilitates the molecular mimicry of advanced logic operations with multiple photonic inputs and outputs. Chemically linked chromophores can exchange information by energy and photoinduced electron transfer processes. This information exchange is a form of logical concatenation.<sup>[37]</sup> For example, light as an input can lead to excited state energy transfer from the absorbing chromophore, which can be a form of logical output. Acceptance of this energy by another chromophore represents an information input. These excited state interactions between the individual

building blocks may be dramatically changed following photochromic reactions, which adds the possibility of controlling energy- and electron transfer processes.<sup>[54]</sup>

These design principles were used by us in 2011 for the photochromic molecular triad FG-DTE (**7**) shown in Scheme 4a.<sup>[53]</sup> The triad consists of two identical fulgimide photochromes (FG) and one dithienylethene photochrome (DTE) covalently linked around a phenyl core. By using light of carefully selected wavelengths in the UV and the visible region of the spectrum, the independent isomerization of the photochromes between the respective open (FG<sub>o</sub> and DTE<sub>o</sub>) and closed forms (FG<sub>c</sub> and DTE<sub>c</sub>) was possible. Hence, isomeric forms, labeled as FG<sub>o</sub>-DTE<sub>o</sub>, FG<sub>c</sub>-DTE<sub>o</sub>, FG<sub>o</sub>-DTE<sub>c</sub>, and FG<sub>c</sub>-DTE<sub>c</sub> were accessible (see Schemes 4b and 5).<sup>[55]</sup> They showed unique spectral features which offered a large selection of optical signatures as outputs in the readout processes. For example, the only fluorescent form is FG<sub>c</sub>-DTE<sub>o</sub>. This is due to the fluorescent nature of FG<sub>c</sub>, in combination with the fact that DTE<sub>o</sub> did not quench the fluorescence by energy transfer, whereas DTE<sub>c</sub> did quench emission. Moreover, with the initial form set as FG<sub>o</sub>-DTE<sub>o</sub> the exposure to 397 nm UV light led to the formation of mainly FG<sub>c</sub>-DTE<sub>o</sub>. Strong fluorescence emission intensity was hence observed upon excitation of FG<sub>c</sub> in this form of the triad. If the sample was subsequently exposed to 302 nm UV light, isomerizing exclusively DTE<sub>o</sub> to DTE<sub>c</sub>, FG<sub>c</sub>-DTE<sub>c</sub> was formed. This form was not significantly fluorescent, as DTE<sub>c</sub> quenched the FG fluorescence by energy transfer. On the other hand, this isomeric form (FG<sub>c</sub>-DTE<sub>c</sub>) had the strongest absorbance at 535 nm, as both FG<sub>c</sub> and DTE<sub>c</sub> displayed substantial absorbance at this wavelength. Exposure of FG<sub>c</sub>-DTE<sub>c</sub> to red light isomerized the triad to the FG<sub>c</sub>-DTE<sub>o</sub> form, and the fluorescence was recovered. From these few examples, it is clear that the use of selective isomerization and distinct spectral features would allow for several combinational and sequential logic operations to be mimicked by the FG-DTE triad.

Indeed, by the use of three photonic inputs in the UV (302 nm, 366 nm, and 397 nm) and two in the visible (green light and red light), together with output readings at five different wavelengths, we showed that the triad can perform the functions of 13 logic devices. These include the half-adder,<sup>[56-58]</sup> half-subtractor, multiplexer,<sup>[16]</sup> demultiplexer,<sup>[15]</sup> encoder,<sup>[18]</sup> decoder,<sup>[18]</sup> keypad lock,<sup>[21]</sup> and reversible logic gates.<sup>[23, 59, 60]</sup> Moreover, all functions were operated with one common initial state (FGo-DTEo), many of them in parallel and all of them resettable by the universal application of green light (see Scheme 5). This complexity is unprecedented at this point of time.

As little attention has been given to sequential logic operations so far in this review article, we will herein focus briefly on the keypad lock function of the FG-DTE triad, rather than giving a comprehensive description of all 13 functions.<sup>[6, 53]</sup> For a combinational logic function such as an AND gate, the state of the output is only dependent on the actual input combination, with no regard to the order in which the inputs are applied. This is not true for a sequential logic function, where the state of the output is sensitive both to the inputs being applied and to the order of application. Sequential logic devices thus have a memory function.<sup>[10]</sup> The keypad lock, such as is commonly found on doors, is an example of a sequential logic device; the inputs have to be applied in the correct sequence for the lock to open, which is equivalent to switching the output to the *on* state.

When operated as the keypad lock (see Scheme 6), the FG-DTE triad has two inputs: UV light at 366 nm and red light. The output is read as the fluorescence of FGc at 624 nm. The initial state is, as for all other operations, FGo-DTEo, to which any isomer of the triad is conveniently reset by exposure to green light. In order to observe intense fluorescence emission from FG, the triad must be isomerized to the FGc-DTEo form. With FGo-DTEo, red light alone has no effect on the isomeric distribution,

whereas the UV light isomerizes the triad to the non-fluorescent FGc-DTEc form. UV light followed by red light, however, results in formation of the fluorescent FGc-DTEo isomer (see Scheme 6), and the output switches *on*. Hence, out of the eight possible ordered input combinations (including the non-activation of an input as a possibility) only “UV = first input, red light = second input” opens the lock.

Seen from a realistic standpoint even sophisticated systems, such as the above discussed all-photonic multifunctional logic platform **7**, are still very far from being a competitive molecular computer model with the functionality of conventional silicon circuitry. However, while a fully functional molecular computer seems ambitious at the time of this Review, it would be clearly a mistake to discard the formulation of such an objective as pure science fiction. Often the path is the aim, and the field of molecular logic is not an exception. In fact, the application of the principles of Boolean algebra for what one could term generally as molecular information processing has already led to applications which no one could foresee when molecular logic emerged *ca.* 20 years ago. The design of intelligent diagnostic devices, therapeutic approaches, and clever materials witness this emerging diversification of the field. The next sections will give a brief overview of these developments.

### **Molecular Logic for Bio-sensing, Diagnostics, and Actuation**

Clinical parameters are in a first approximation often evaluated intuitively by binary reading, i.e., the measured value is above or below a certain reference value. Moreover, a physician combines this YES/NOT information intuitively with simple logic functions like AND or OR and arrives at a first diagnosis. In this context, the possibility to treat complex analytical situations through the combination of multiple parameters by a logic

operator and thus translate them into a single readable output (for example a fluorescence signal), is a very attractive tool for clinical analysis.

In 2006 Magri and de Silva reported a 3-input fluorescent AND gate **8** (see Scheme 1)<sup>[61]</sup> which works based on the same principles of enabling or blocking photoinduced electron transfer (PeT) fluorescence quenching as discussed for the first molecular logic gate by de Silva *et al.* in 1993.<sup>[11]</sup> The design included anthracene as central signaling fluorophore and three selective receptors for H<sup>+</sup>, Na<sup>+</sup>, and Zn<sup>2+</sup>. Only when all three receptors were blocked and hence, all quenching pathways (PeT) were switched *off*, was the highest fluorescence output at *ca.* 430 nm observed. The fluorescence enhancement factor for this “all inputs present” situation was *ca.* 3-6 in comparison to all other input combinations. This output signal differentiation was sufficient to allow the unambiguous identification of the simultaneous presence of all three chemical species.

Meanwhile, the idea of applying logic operations for differentiation between clinical situations has started to attract more and more research groups. In the following paragraphs we will concentrate on logic devices with enhanced value for the analytical evaluation of critical parameters characteristic for specific diseases. In this context Margulies and Hamilton published in 2009 an approach to interpreting combinations of simple logic operations in the form of YES, NOT, and PASS 1 for the identification of different concentration levels of proteins.<sup>[62]</sup> One example is the myelin basic protein (MBP), which is typically overexpressed in the cerebrospinal fluid of multiple sclerosis patients. A mixture of G-rich DNA quadruplexes, modified with three fluorophores (pyrene, fluorescein, and tamra), was applied for this purpose. The fluorophores were selected for their emission spectra, which are sufficiently distinct to produce unique spectral patterns (analyzed as outputs), depending on the nature and concentration of the

input protein which interacts with the DNA quadruplexes. In the reported case the output was detected at 525 and 590 nm, yielding for MBP the combination of a NOT and PASS 1 gate, respectively. At  $[MBP] \geq 750$  nM the emission output vector was observed as 01 (525/590 nm), while below this limit a 11 vector was read. Control proteins like avidin and melittin gave distinct logic gate combinations for these two emission channels and thus, could be safely differentiated from MBP.

Konry and Walt described in 2009 a useful platform for the combinational fluorescence sensing of bacterial DNA and a pro-inflammatory cytokine (IL-8 protein).<sup>[63]</sup> The presence of both biomarkers is a typical situation for bacterial respiratory infections. A system was developed, which responded by a combination of an AND and an INH operation; see Scheme 7. For this purpose microspheres modified with monoclonal antibodies were used to recognize the cytokine protein (input In1 in Scheme 7). A secondary antibody, labeled *via* an avidin-biotin pair with a capture probe DNA, was then linked to the cytokine. The bacterial DNA input (input In2 in Scheme 7) hybridized to the capture probe and to a signal probe oligonucleotide with a fluorescent Cy3 dye tag (fluorescence output of the AND channel). A second Cy5-tagged signal probe sequence (fluorescence output of the INH channel) was designed to bind to the capture probe DNA in absence of the DNA input. In consequence of this supramolecular design the following situation was observed: when no input (DNA or protein) was present no fluorescence was observed for either channel (Cy3 or Cy5). When only DNA input was present and protein was missing, no binding to the microsphere was achieved and a low fluorescence signal was measured for both dyes. However, when protein was present, but when DNA was absent the Cy3 signal was low (AND channel) and the Cy5 signal read high (INH channel). Finally, when both inputs were applied and the DNA concentration was sufficiently high to saturate all capture

probe DNA, the opposite observation was made: a high Cy3 signal and a low Cy5 emission. Hence, AND and INH gate functions were operated in parallel. With this approach samples with a high IL-8 protein concentration caused by a bacterial infection (presence of bacterial DNA) can be unambiguously differentiated from false positives, i.e., samples with high IL-8 expression that is not caused by the action of bacteria.

In 2010 the Katz group reported a series of enzyme-based systems for the combinational logic detection of a series of biomarkers indicative for several types of lesions.<sup>[64]</sup> For example, high concentrations of alanine transaminase (ALT) and lactate dehydrogenase (LDH) are indicative of severe liver injury. These two enzymes were used as inputs to a biocatalytic cascade system (see Scheme 8). ALT converted  $\alpha$ -ketoglutarate into glutamate and alanine into pyruvate. The latter, on the other hand, was a substrate for LDH, which converted it into lactate under simultaneous oxidative transformation of NADH into  $\text{NAD}^+$ . The absorbance of NADH at 340 nm was measured as the optical output of the system. A solution containing NADH and the two mentioned substrates for ALT will have the cascade working only in the simultaneous presence of both enzymes, leading in consequence to a diminished absorption signal of NADH due its oxidation to  $\text{NAD}^+$ . This corresponds to a NAND gate (to be interpreted as an output-inverted AND gate). An array of six enzyme cascade logic gates (four AND gates and two NAND gates) was assembled, and one of them was the ALT/LDH system discussed. Each gate corresponded to a specific type of lesion: soft tissue injury, traumatic brain injury, liver injury, abdominal trauma, hemorrhagic shock, and oxidative stress. With this array a specific binary code for single or multiple injuries was generated by adopting a multiplexing strategy. The work shows in an impressive way that relatively simple enzymatic logic operations can yield increased levels of

complexity when integrated in a gate library and thus, may provide valuable information for injury diagnosis.

It would be a step forward if the diagnostic output could be translated into an actuation mechanism in the form of the release of a corresponding therapeutic agent. An approach to this was reported by the Katz group, building on their experience with enzyme logic systems and the transduction of a chemical response into an electrochemical signal.<sup>[65]</sup> The above discussed cascade of ALT- and LDH-catalyzed processes was integrated with the transformation of glucose into gluconic acid by glucose dehydrogenase in presence of  $\text{NAD}^+$  as a cofactor. The formation of gluconic acid was accompanied by a pH increase, which de-blocked an ITO electrode modified with a pH-responsive polymer (see below the section on intelligent materials for another use of this polymer). The activated electrode could then take part in electron transfer with  $\text{Fe}(\text{CN})_6^{4-}$ , yielding the observation of electrochemical output signals (e.g., in cyclic voltammetry). In summary, the simultaneous presence of ALT and LDH was translated into an electrochemical signal, which depended on a pH change. This is still far from a biologically relevant actuation mechanism, but it shows a way to actually utilize a logically-motivated chemical output of an enzymatic cascade.

The idea of coupling the response of biomarker signal processing to the release of a drug molecule, thereby creating a therapeutic and diagnostic (theranostic) device, has been followed by Shapiro and Benenson. In 2004 they published a biomolecular computer which processed specific mRNA indicators *in vitro*, leading to the release of a drug molecule in case of a positive diagnosis.<sup>[66]</sup> In a concrete example, genes related to prostate cancer (PPAP2B/GSTP1 underexpression and PIM1/hepsin overexpression) triggered the release of a short single stranded DNA (GTTGGTATTGCACAT) which is known to inhibit the synthesis of MDM2 protein by binding to its messenger RNA.

MDM2 is a negative regulator of the p53 tumor suppressor. The formal logic circuit shown in Scheme 9a summarizes the mRNA input-dependent drug release. In practice, each gene concentration level (overexpression or underexpression) was analyzed by a molecular automaton (Scheme 9b) in a YES/NO fashion with respect to the typical levels associated to prostate cancer. The initial situation was a positive state (YES) of the automaton. As long as the system stayed in a YES state (or binary 1), corresponding to the correct concentration levels of the four mRNA genes, the positive diagnosis string was followed. This led to high drug concentrations (Out = 1). Once an input concentration level was identified as mismatching, the NO string was followed. This resulted in the release of a drug suppressor and thereby a low drug concentration (Out = 0).

In 2011, Benenson and Weiss showed that the actuation of a classifier circuit in combination with specific expression levels of a set of six microRNAs can trigger a cellular response in form of apoptosis.<sup>[67]</sup> The logic circuit shown in Scheme 10 takes into account that some of the microRNA biomarkers found in HeLa cancer cells are overexpressed while others are underexpressed. Only when all biomarkers were encountered in their corresponding concentration level, which differentiates HeLa cells from healthy cells, was the output protein hBax expressed. This protein led to cell apoptosis. Hence, sensing or diagnosis was coupled to an actuation process, which is conceptually related to the above discussed work by Shapiro and Benenson. The last two works clearly show that the concepts of molecular computation are, when cleverly integrated in biomolecular networks, a very promising tool toward novel theranostic strategies with enhanced selectivity and possibly reduced side effects. In the following section more systems along the lines of drug delivery and activation will be discussed, with the focus on pro-drug activation.

## Molecular Logic for Pro-Drug Activation and Drug Delivery/Release

One of the most promising areas for the exploitation of molecular information processing is the application of binary logic for the “intelligent” delivery of drug molecules. The last two systems discussed in the preceding section are prime examples. One way to achieve target-specific drug delivery is the integration of selective recognition sites in the drug molecules, which allow their exclusive supramolecular interaction with structures associated with a certain clinical malfunction or disorder. This approach requires a delicate fine-tuning and understanding of the manifold interactions of a drug with receptors. However, very often biomolecular structures which are affected by illness feature a significant variation of environmental parameters (pH and concentrations of physiologically important cations) with respect to healthy tissue. This differentiation may be used to activate a pro-drug or to release a drug under very specific conditions. The binary logic combination of several environmental factors enhances the possibility for very selective drug delivery and minimization of undesired side effects. In combination with light as an external input factor not only spatial (where) but also temporal (when) control can be potentially implemented as additional asset.

In 2009 the group of Akkaya reported a very interesting example related to the multiparameter-dependent generation of singlet oxygen,  $^1\text{O}_2$  (Scheme 11).<sup>[68]</sup> Singlet oxygen is the effective agent of photodynamic therapy (PDT), and is generated by a photosensitized transformation of ground state triplet oxygen  $^3\text{O}_2$  as a pro-drug. A boron-dipyrromethene (BODIPY) dye **9** with pyridylethenyl substituents in the 3- and 5- positions and a benzo-5-crown-15 in 8-position was used as sensitizer (Scheme 11). The protonation of the pyridyl substituents led to a perturbation of the internal charge transfer (ICT) system, which was expressed by a 30 nm red shift of the long-wavelength

absorption band of the BODIPY dye. The shifted absorption maximum rendered the dye capable of excitation with a 660 nm LED array. The BODIPY excited singlet state underwent intersystem crossing to the triplet state, which is capable of sensitizing the formation of singlet oxygen. However, the triplet yield of the dye is diminished by the action of intramolecular photoinduced electron transfer (PeT), which competes with intersystem crossing of the excited singlet state. The electron-donating benzo-5-crown-15 is responsible for the photoinduced electron transfer, and can be deactivated by complexation of Na<sup>+</sup> ions. Hence, the simultaneous presence of H<sup>+</sup> (low pH) *and* Na<sup>+</sup> ions favored the excited triplet state formation of **9** and thereby the sensitization of singlet oxygen. This system corresponds to an AND logic gate using two chemical inputs and generating a useful output in the form of a cytotoxic agent. Akkaya and co-worker found that the rate of singlet oxygen formation was enhanced by factors of 2 to 6 in comparison with the absence of both inputs or the presence of only one input. The clever photophysical design and realization of this “intelligent” photosensitizer is a proof-of-principle demonstration, which coincides qualitatively with the physiological conditions of tumor tissue where lower pH and higher Na<sup>+</sup> concentrations as compared to healthy tissue are frequently found. However, it was pointed out by the authors that the required high concentrations of the chemical activators of the AND logic gate are not compatible with real clinical situations.

The Shabat group showed in 2005 a different case of pro-drug activation, where the drug component was caged in a conjugate (the pro-drug **10**) containing substrate triggers for penicillin G amidase (PGA) and catalytic antibody (Ab) 38C2 (see Scheme 12).<sup>[69]</sup> The action of each of these two enzymatic inputs created a primary amino group, which in an intramolecular nucleophilic attack at a carbamate-containing linker, followed by 1,6-elimination, released the doxorubicin anticancer drug. The system

followed OR logic behavior, because each single input as well as their simultaneous presence yielded the free drug. It was found that the  $IC_{50}$  values, obtained from cell growth inhibition assays (MOLT-3 and HEL cells), are quite comparable to those obtained for the direct administration of the drug. This work is a clever extension of works where single enzymes with significant overexpression in tumor tissue were used to release the therapeutic cargo of a pro-drug. In the case of **10** the combination of two enzymes *via* a logic operator creates higher chances for selective actuation.

Until now we have had a look at logically operated pro-drug activation by processing exclusively chemical information. In terms of spatiotemporal control the use of light signals may offer advantages for selective drug delivery. In 2010 the Andréasson group reported the exploration of the photoionic switching between the three states of a cationic spiropyran (spiro form **11-SP**, merocyanine form **11-ME**, and protonated merocyanine form **11-MEH<sup>+</sup>** (Scheme 13)).<sup>[70]</sup> The **11-SP** form (pro-drug) was converted to the colored merocyanine **11-ME** (drug) by irradiation with UV light, while the reverse isomerization was initiated by visible light irradiation. The protonated merocyanine **11-MEH<sup>+</sup>** was generated by protonation of the **11-ME** form. This process can be reverted by addition of a base or exposure to visible light. At pH 7 the spiro form **11-SP** is rather stable, except for a slow minor ring opening (10 % **11-ME** in the equilibrium, time constant *ca.* 75 min) and an even much slower subsequent irreversible hydrolysis reaction (time constant *ca.* 80 h). Irradiation of an aqueous solution of **11-SP** at pH 7 with 254 nm light triggered the photochromic ring opening (35% **11-ME** in the photostationary state) and no protonated merocyanine **11-MEH<sup>+</sup>** was formed ( $pK_a$  of the phenolic oxygen is *ca.* 4.5). Addition of calf-thymus DNA did not lead to significant changes of the absorption spectra at pH 7. At pH 6 and in absence of DNA the same observations are made for the photochromic behavior of **11-SP**. However, in the

presence of the biomolecule a significant binding of the photochrome in the  $\text{MEH}^+$  form was observed. While  $\mathbf{11}\text{-MEH}^+$  was virtually nonexistent (*ca.* 3 %) at pH 6, the addition of DNA shifted the protonation equilibrium, which is a case of complexation-induced protonation. The binding of  $\mathbf{11}\text{-MEH}^+$  was favored over  $\mathbf{11}\text{-MC}$  due to the neutralization of the negative charge, which would induce electrostatic repulsion with the negatively charged DNA backbone. In summary, the photoionic activation of the  $\mathbf{11}\text{-SP}$  pro-drug follows the logic AND operation: only in the presence of UV light and at pH 6 is significant drug binding observed. A small drop of pH by one unit coincides with the differentiating conditions of tumors *versus* healthy cells. Thus, the presented system combines realistic clinical conditions with spatiotemporal control of pro-drug activation by photonic stimuli. Interestingly, a recent live cell study by the Andréasson group showed that spiropyrans have indeed potential as light-activated drugs.<sup>[71]</sup>

Another interesting case of light-activated drug delivery was introduced by Aida and co-workers, who reported in 2006 a genetically modified GroEL molecular chaperon which was decorated with photoisomerizable azobenzene switches (Scheme 14).<sup>[72]</sup> Chaperones are proteins that play an important role in the control folding/unfolding of biological macromolecular structures. In the present case green fluorescent protein (GFP) was chosen as model drug for loading the cavity of the GroEL structure. Native GFP is highly fluorescent ( $\lambda_{\text{max}} = 511 \text{ nm}$ ), while its denaturated form is non-fluorescent. It was noted that the GroEL in its closed form (absence of adenosine triphosphate ATP as a cofactor) did not permit re-folding of denaturated GFP. GroEL can be opened in the presence of ATP (In1). While GFP could be released in principle from the open GroEL, the portal azobenzene units in their *trans*-form slowed down the release rate by a factor of *ca.* 3. Hence, a second input was constituted by 350 nm light (In2), which caused the *trans*-azobenzene to photoisomerize

to the *cis*-form. Only upon the simultaneous application of both inputs with the supramolecular *trans*-azo-GroEL<sub>closed</sub>/GFP<sub>denaturated</sub> assembly, was the fastest GFP release observed. The system is a kind of “semibiological molecular machine” with AND logic behavior and a fluorescence output signal. The reversible nature of the azobenzene photoisomerization (*cis-trans* isomerization by irradiation with visible light,  $\lambda > 400$  nm) can be exploited to switch at will between fast and slow release in the presence of ATP, as was shown in the original report. Other guests can be imagined for this approach, which makes the described photo-gated GroEL chaperone an interesting container for “intelligent” drug delivery.

In general the combination of light-induced supramolecular switching with a chemical cofactor provides interesting case studies with potential for intelligent and spatiotemporally resolved drug delivery. In 2011 the Pischel group reported the release of the Hoechst 33258 dye (**12**; Scheme 1) from its supramolecular complex with the macrocyclic cucurbit[7]uril (**13**; Scheme 1) by actuation of a photoinduced relay mechanism in form of a pH jump.<sup>[73]</sup> The photoinduced change of the pH from 7 to 9 triggered a drop of the guest binding constant by two orders of magnitude ( $1.7 \times 10^6$  M<sup>-1</sup> versus  $2.8 \times 10^4$  M<sup>-1</sup>). Hoechst 3328 is known to exhibit anthelmintic activity and actuates as helicase and topoisomerase inhibitor. Cucurbiturils are known to bind a large spectrum of cationic organic guests and also alkali metal ions (e.g., Na<sup>+</sup> ions), which may also induce drug guest release due to guest competition. This would ultimately lead to an OR gate (monitoring the drug release as output) triggered by photonic signals and chemical inputs. Indeed, the usefulness of cucurbiturils for the realization of supramolecular logic operations has been demonstrated.<sup>[74]</sup>

In 2009 the groups of Stoddart and Zink published a very interesting approach toward drug delivery which responds according to AND logic.<sup>[75]</sup> They combined their

conceptual approach of mechanized silica nanoparticles with pH- and light-responsive functionalities (Scheme 15). The nanoparticles were modified at the pore entrances with bisammonium stalks, which form supramolecular complexes with cucurbit[6]uril (CB6; an analogue of cucurbit[7]uril shown in Scheme 1). This led to the blocking of the mesopores, such that cargo contained in the pores was retained. The cucurbituril macrocycles were removed by deprotonation of the ammonium groups upon addition of base (sodium hydroxide in this case). The inside walls of the pores were modified with photoaddressable azobenzene units. As discussed above, these can be interconverted between their *cis* and *trans* forms by irradiation with UV and visible light. However, using light of a wavelength where both isomers absorb (448 nm) triggers a wagging motion which facilitated the removal of the cargo. Only when both inputs (base and 448 nm light) were activated was an efficient cargo release observed, as was monitored using a fluorescent guest [ReCl(CO)<sub>3</sub>-2,2'-bipyridine] as a drug model. This example illustrates the interest of molecular logic in the context of drug delivery and materials chemistry.<sup>[76]</sup> More examples for the logic switching of materials will be discussed in the following section of this Review.

### **Molecular Logic for the Conception of Intelligent Materials**

Two approaches will be discussed and illustrated: a) the switching of materials' properties based on binary logic operations and b) the integration of molecular logic devices into organic matrices (polymers/gels) or their grafting onto inorganic/organic materials.

Considerable efforts have been dedicated to the switching of the physical properties (optical spectra, size, *etc.*) of nanoparticles either by controlling their aggregation/deaggregation or the ionization state of capping ligands. In 2003 the Aida

group reported an example where the photoluminescence of CdS quantum dots nanoparticles was reversibly switched by controlling the input-dependent conformation of the GroEL chaperone protein.<sup>[77]</sup> This protein was discussed already in the preceding section in the context of drug delivery by chemical and photochemical switching. Aida and co-workers used the protein cavity to encapsulate CdS nanoparticles and in agreement with their electronic insulation a strong luminescence signal was observed. The protective role of the protein was also evident by the much less efficient nanoparticle luminescence quenching *via* photoinduced electron transfer to the strong electron-accepting methylviologen (15-35 times less efficient quenching in the chaperone-CdS complex as compared to the free nanoparticle). Chaperones are known to change their conformation and to allow the release of encapsulated cargo to the bulk solution upon binding of  $Mg^{2+}$  and ATP, which can be defined as chemical inputs. The sole of addition of either input had no effect on the chaperone-CdS complex. However, the simultaneous presence of  $Mg^{2+}$  and ATP led to nanoparticle release and subsequent coagulation. This was accompanied by a practically quantitative reduction of the luminescence signal (output signal). Although this behavior was not interpreted in terms of molecular logic in the original report, it is easily identified that it parallels that of a NAND gate (high luminescence for all input combinations except when both chemical signals were coded by a binary 1).

With a similar objective Lu and co-worker described in 2006 a series of clever systems which made use of supramolecular assembly/disassembly of oligonucleotide-modified gold nanoparticles.<sup>[78]</sup> Complementary DNA sequences with integrated aptamers, responsive to adenosine, cocaine, or  $K^+$ , were incorporated into the nanostructures. With this conceptually innovative approach AND and OR logic gates were implemented. The state of aggregation of the nanoparticles was read by

monitoring the concomitant changes in the optical spectrum, also detectable by color changes visible to the naked eye. While aggregated, the gold nanoparticles exhibited a broad absorption band in the visible spectral range extending beyond 700 nm. The input-dependent dispersion of the nano-objects was monitored by the appearance of a much sharper and more intense plasmon band with a maximum at 522 nm and a considerably lower absorbance in the 700 nm region. To provide a clear-cut output reading the authors chose the absorbance ratio between 522 nm and 700 nm. In a very recent work, Tan and co-workers used input (ATP, cocaine) recognition by designed aptamers for triggering structural modifications in crosslinked hydrogels and thereby provoking gold nanoparticle release.<sup>[79]</sup> The output as a function of binary AND or OR logic was followed by changes in the optical spectra of the nanoparticles. The authors stressed that their approach is versatile in that other cargo, such as drug molecules, could be integrated into the material.

In 2010 Zhang and co-workers showed that the cooperative action of metal ion inputs ( $Mg^{2+}$  and  $Pb^{2+}$ ) as cofactors of catalytically active oligonucleotides, so-called DNAzymes, can be used for the design of colorimetric logic gates.<sup>[80]</sup> The output was, again defined by typical spectral changes in the plasmon band region of gold nanoparticles. The action of the DNAzyme led to the scission of a circular DNA substrate equipped with cleavable ribonucleobases and complementary sequences for hybridizing to the DNAzymes. Once the circular structure was cleaved, oligonucleotide-modified gold nanoparticles were bound to the open structure, which served as a means to aggregate the particles. In this way, by reading the spectral output as UV/vis absorption changes, OR, AND, and INH gates were demonstrated for different combinations of circular substrates and DNAzymes.

Bhatia and co-workers presented in 2007 an interesting strategy for detecting the combinational activity of two matrix-metalloproteinases (MMP2 and MMP7) through monitoring the assembly of superparamagnetic  $\text{Fe}_3\text{O}_4$  nanoparticles (Scheme 16).<sup>[81]</sup> The relevance of the results is underlined by the role of MMP2 as a biomarker for cancer invasiveness, metastasis, and treatment efficacy, while MMP7 plays a role in mammary carcinoma progression. The nanoparticles were decorated with biotin or neutravidin, which can form an ultrastable supramolecular guest-receptor complex, working as “nanoparticle glue”. However, the additional surface functionalization with protease-specific (MMP2 or MMP7) oligopeptide substrates having a polyethylene glycol (PEG) tail blocked the supramolecular interaction and consequently no nanoparticle aggregation was observed. Depending on the design principle, AND or OR logic operations with the proteases as inputs and the measurement of the hydrodynamic radius of the iron oxide nanoparticles as output were designed. Also the T2 relaxation rate was amplified by the nanoparticle aggregation, which was used for magnetic resonance imaging (MRI) information processing. As shown in Scheme 16, the tailored functionalization of each type of nanoparticle (either modified with biotin or neutravidin) with a substrate polymer specific for MMP2 or MMP7 enabled AND logic. On the other hand, the tandem functionalization of one type of nanoparticle with both peptide substrates yielded OR logic. The results have much interest for the exploitation of combinational logic for the monitoring of typical enzymatic markers linked to tumorigenesis.

In 2008 Katz and co-workers reported the realization of nanostructured ensembles composed of enzyme-decorated silica microparticles and signal transducing gold-coated magnetic nanoparticles with a cobalt ferrite core ( $\text{CoFe}_2\text{O}_4$ ); see Scheme 17.<sup>[82]</sup> The magnetic properties were explored to keep the particles in solution while an

external magnetic field was applied. The immobilized enzymes were chosen to respond in the logic framework of AND or OR operations to various substrate inputs with a change of pH (output). In turn the pH sensitivity of mercaptopropionic acid capping ligands on the signal transducing gold-coated magnetic nanoparticles was used to translate the pH changes into a shift of the localized surface plasmon resonance (LSPR) band of the gold shell. The AND logic was realized by using a combination of input processing silica microparticles with covalently linked invertase (Inv) and glucose oxidase (GOx). The substrate of Inv was sucrose (In1), which was converted into glucose. This product was subsequently transformed into gluconic acid by the action of GOx in the presence of oxygen (In2). Hence, the enzymatic cascade led only to gluconic acid when the necessary inputs sucrose and oxygen were provided, which is compatible with AND logic. The formed acid lowered the pH of the solution (from pH 7 to pH 4 under the chosen experimental conditions) and in consequence the capping ligand of the gold shell of the magnetic nanoparticles was protonated. This was accompanied by a red shift of the LSPR band by *ca.* 21 nm. Often these shifts are interpreted as the result of a nanoparticle aggregation (see above). However, in this case it was demonstrated that instead the LSPR energy of the isolated nanoparticles was influenced by the change of the ionization state of the capping ligands. In the same work also an OR logic system was devised. The use of GOx and esterase (Est) allowed the transformation of glucose (in the steady presence of oxygen) to gluconic acid and of ethyl butyrate to butyric acid, respectively. Hence, a drop in pH was initiated by each substrate or both substrates simultaneously, as required by the OR operation. It is of interest to achieve resettable logic operations, for which the authors employed urease-modified silica microparticles. With this system urea is biocatalytically transformed into ammonia, resulting in a pH

increase (back to the initial neutral level, pH 6.5–7.0) and the consequent observation of an inversion of the spectral shifts.

In another work, also published in 2008, the Katz and Minko groups proposed the switching of the assembly/disassembly of pH-responsive polymer-modified silica nanoparticles by functional coupling with identical enzyme logic AND/OR systems as described in the preceding paragraph (now the enzymes being the inputs for the substrates, but without formal consequences for the logic operation).<sup>[83]</sup> Specifically, poly-2-vinylpyridine was grafted onto silica nanoparticles (200 nm). It was found that at pH < 5, where the charged (protonated) polymer was predominant, the nanoparticles were in a dispersed state. At pH > 5 the hydrophobic interactions of the uncharged polymer chain became important and nanoparticle aggregation was observed. The assembly/disassembly was monitored by dynamic light scattering and scanning probe microscopy. The information processing of the enzyme logic system resulted in a pH decrease, leading to nanoparticle disassembly. Running of the urea/urease reset mechanism caused a pH increase and nanoparticle assembly. In essence, pH changes as the result of logic operations were transduced into changes of properties of a nanoparticle suspension. Although no direct application was associated with the results, it was suggested that they may serve for logic control of liquid flow in microfluidic devices.

In most examples discussed above information processing was performed with nanostructured systems, monitoring nanoscopic properties. However, for some applications it may be actually desirable to achieve truly macroscopic changes in a size range visible to the naked eye. Well defined three-dimensional size changes in the millimeter range were discussed in a series of reports about chemomechanical polymers developed by the Schneider group.<sup>[84]</sup> These polymers contain various functional

recognition sites for effector molecules, which are attracted *via* ion-pairing, hydrogen bonding, cation- $\pi$  interactions, metal complexation, hydrophobic effects, *etc.* (see two example polymers in Scheme 18). In the case of two inputs, positive cooperativity may be observed, which relates directly to an AND logic operation. Several cases of chemomechanical AND gates were discussed in the literature.<sup>[85, 86]</sup> For example, for an ethylenediamine-containing polymer it was found that volume expansion is promoted by short peptides and aminoacids only in the presence of metal ions such as  $\text{Cu}^{2+}$  or  $\text{Zn}^{2+}$ .<sup>[86]</sup> The effect has been explained in terms of the formation of a ternary complex between the diamine ligand and the two chemical inputs: the metal cation and the peptide/amino acid. Each input alone led to lower volume expansions. Similar observations were made for the same polymer in combination with adenosine monophosphate (AMP) and phosphate anionic effectors.<sup>[85]</sup> A system with logic NAND behavior was realized with a polyethylenimine, which favors supramolecular recognition *via* ion pairing and cation- $\pi$  interactions. With 2-naphthoate and amino acids as effectors the largest volume contraction (binary 0) was observed for their simultaneous presence.<sup>[87]</sup> The Schneider group delivered proof-of-principle for the utility of chemomechanical polymers as actuators (machines) or in drug delivery.<sup>[84]</sup> This application potential together with the demonstrated logic switching opens interesting perspectives for the further career of these “intelligent” materials.

In a related work, the chemically-induced shrinking/swelling of a hydrogel membrane was exploited by the Katz and Minko groups in 2009.<sup>[88]</sup> The application of their above discussed enzymatic AND and OR logic gates led to pH changes. These were transduced into morphological changes of a pH-responsive alginate/gelatin hydrogel. The structure is comprised of *D*-mannuronic acid and *L*-guluronic acid moieties cross-linked by  $\text{Ca}^{2+}$ . At  $\text{pH} < 4$  the acids are in their charge neutral state,

corresponding to the shrunken state of the hydrogel membrane with permeable pore structure. On the other hand, at  $\text{pH} > 5$  the carboxylic acid groups were deprotonated, swelling was observed, and the membrane pores were closed, which resulted in a much less permeable polymer. The membrane state was characterized by measuring the electron transfer resistance of the membrane deposited on an electrode surface and also by observing the permeability for a fluorescent dye (rhodamine B). Again, the association of the enzyme-responsive logic gates (AND/OR) with structural changes of a membrane may have interesting applications for controlling drug delivery.

Up to this point the application of molecular logic switching for changing properties of materials has been discussed. A different strategy is the use of materials as supports for discrete molecular logic devices. Along this line of thought in 2006 the de Silva group immobilized several ion-responsive fluorescent molecular logic gates (containing anthracene or pyrene signaling units) on Tentagel-S-NH<sub>2</sub> polymer beads.<sup>[89]</sup> Each device was chosen to give a fluorescence response to an H<sup>+</sup> input in form of YES, NOT, PASS 1, and PASS 0 logics. Already with these few combinations the authors were able to show the usefulness of logically-responsive fluorescent tags for coding micro-objects, which is a central topic in combinatorial chemistry. The simple combination of various excitation and emission colors, logic types, and input types leads to a conservative estimation of *ca.* 3500 possibilities for different tags. When this approach is combined with multivalued logic, which distinguishes signal values beyond 0 and 1, approximately 31 million different tags can be produced. Combinatorial chemistry relies heavily on clever strategies for coding resin pearls which are used as solid supports for the construction of large product libraries. Among the most successful approaches are labeling with radiofrequency chips, chemical encoding coupled to mass spectrometric detection, and optical encoding with fluorophores.<sup>[90]</sup> The combination of

fluorescent tags with principles of binary and multivalued logic adds clearly another layer of complexity to these approaches.

Other materials used for the immobilization of fluorescent molecular logic gates include silica nanoparticles and silica nanowires.<sup>[91, 92]</sup> Raymo and Giordani reported the example of a silica-monolith-caged spiropyran photochromic switch which functionally integrates a sequential logic function.<sup>[93]</sup> Matsui and Sugimoto demonstrated the use of molecularly imprinted polymers for the purpose of mimicking logic operations.<sup>[94]</sup> The anchoring of molecular logic gates onto glass surfaces or electrodes has been followed up by many groups. The efforts of the van der Boom group in this field have led to a series of molecular logic gates and molecular memory devices with set-reset characteristics.<sup>[28, 29]</sup> Their approach built on the exploitation of the versatile redox chemistry of organometallic osmium and ruthenium complexes.<sup>[39]</sup> A resume of these works has been published recently.<sup>[30, 31]</sup> Also the decoration of electrode surfaces with (macro)molecular entities fits in this collection of examples where the material is either an inert bystander or a means to deliver/read signals related to the logic switching. For example, gold electrodes have been modified with electroactive photochromic switches (set-reset latches),<sup>[27]</sup> electrochemically-addressable rotaxanes and catenanes,<sup>[95-97]</sup> and Langmuir-Blodgett films of co-polymers with chromophores, electron donors, and acceptors for photocurrent generation (AND and XOR gates).<sup>[98, 99]</sup> Titanium dioxide electrodes were functionalized with inorganic, organic, and organometallic species to make use of the photoelectrochemical photocurrent switching effect for implementing various logic gates (e.g., OR and XOR for  $[\text{Fe}(\text{CN})_6]^{4-}@\text{TiO}_2$ ).<sup>[100, 101]</sup>

While in the preceding examples fluorescence switching was achieved with immobilized fluorophores, Callan and co-workers introduced in 2010 a system where the fluorescence emission of the material itself was read as the output signal of a logic

operation (Scheme 19a).<sup>[102]</sup> In detail, the surface of a green-fluorescent CdSe/ZnS core-shell quantum dot was modified with two electron donors (aniline and an azacrown ether). In their activated state these donors led to a pronounced fluorescence quenching of the quantum dot. Akin to the demonstrated working principle of purely organic molecular logic AND gates (see the abovementioned example of the first published molecular logic gate by de Silva *et al.* in 1993),<sup>[1]</sup> only the simultaneous deactivation of both electron donors by binding of H<sup>+</sup> (aniline) and Na<sup>+</sup> (azacrown) switched the fluorescence output *on* (Out = 1). Any other binary input combination (absence of inputs or presence of only one input) left the emission signal low, corresponding to Out = 0.

In a work published by the Willner group in 2009, core-shell CdSe/ZnS quantum dots of different size and emission colors were surface-modified with thymine-rich or cytosine-rich oligonucleotides which showed selective recognition of redox-active transition metal cations such as Hg<sup>2+</sup> or Ag<sup>+</sup>, respectively (Scheme 19b).<sup>[103]</sup> Upon metal ion recognition the quantum dot luminescence was quenched by photoinduced electron transfer (PeT), corresponding to a simple NOT logic operation. The “cocktail” combination of differently modified quantum dots showing two emission output colors (560 nm and 620 nm) opened a way to implement AND and OR logic functions with metal cationic inputs. Again, as observed for the preceding example, the quantum dot was integrated as a signaling building block in the logic devices.

Organogels with integrated photochromic units can be switched by temperature control of sol-gel transition and light-induced isomerization. If this is combined with a fluorescence response in function of the binary application of these two input parameters, logic operations can be potentially interpreted. Tian and co-workers reported in 2006 a system based on the organogelator **14** with integrated fluorophore

(derived from naphthalimide) and photochrome (dithienylethene) units; see Scheme 20a.<sup>[104]</sup> However, no concrete logic operation was connected to the thermal and photochemical switching of the system. Three years later, in 2009, Park and co-workers reported the light- and temperature-induced switching of a mixed fluorescent organogel, composed of the compounds **15** and **16** (Scheme 20b).<sup>[105]</sup> The fluorescent organogelator **15** showed the phenomenon of aggregation-induced enhanced emission ( $\lambda_{\text{fluo,max}} = 575 \text{ nm}$ ) in the gel state. The transition to the sol state was triggered by heating and a dramatically reduced fluorescence was observed. The dithienylethene photochrome **16** was isomerized by irradiation with 300 nm UV light to its closed colored form ( $\lambda_{\text{abs,max}} = 580 \text{ nm}$ ), which showed a large spectral overlap with the organogelator emission and thereby led to highly efficient fluorescence quenching by intermolecular Förster resonance energy transfer. The system can be reset by cooling and irradiation with visible light ( $\lambda > 450 \text{ nm}$ ). The authors defined the fluorescence quenching as output and the gel with the photochrome in its open form (no fluorescence quenching) was the initial state. Heating or UV irradiation or both inputs applied simultaneously led to emission quenching, corresponding to an OR logic operation. In a more direct way the fluorescence signal could be read (high fluorescence corresponds to a binary 1 and low fluorescence to a binary 0) and then the complementary NOR logic gate would result. The potential of the system to act as a molecular memory was also demonstrated.

In 2004 Uchiyama, Iwai, and colleagues reported the innovative design of a thermo- and pH-responsive co-polymer **17** (Scheme 21), which was read through the emission of an appended benzofurazan-type fluorophore.<sup>[106]</sup> The fluorescence of the latter is highly dependent on its microenvironment, showing higher quantum yields in less polar media. The polyacrylamide backbone constituted the temperature-sensitive

part of the co-polymer, leading to a decrease of the microenvironmental polarity near the fluorophores with increasing temperature. Furthermore, part of the polyacrylamide contained a pH-sensitive amino function, which upon protonation influences the hydrophilicity/hydrophobicity balance of the polymer chain and consequently its temperature response. This explained the observation of a lack of temperature-dependent fluorescence at pH 5, while at pH 9 the fluorescence quantum yield increased by a factor of *ca.* 9 upon heating from 10 °C to 35 °C. In other words; high temperature and high pH were required to observe the highest fluorescence response, which was correctly described by binary AND logic.

### **Summary and Outlook**

For nearly 20 years, molecules that mimic the functions performed by silicon-based logic devices have been designed and characterized. What started out with the simple and intuitive molecular AND gate has now developed into unimolecular species capable of performing a large selection of advanced logic functions common to conventional microprocessor circuits. Still, there is no competitive molecular computer and several barriers must be overcome before the research field will develop from the “proof-of-principle” stage to the creation of ready-to-use devices. The concatenation problem remains to be solved with a general approach, and solid state platforms must substitute the solution-based chemistry that dominates today. As discussed in this Review, all-photonic systems may be considered a step in the right direction, because they can be operated in rigid media and, at least formally, overcome the input-output inhomogeneity barrier closely related to the concatenation problem.

However, molecular information processing is much more than just the effort of replacing conventional electronic computers. This is manifested in systems designed to

be functional in “wet” milieus. The sensing, probing, diagnostics, and actuation in biological systems profits clearly from the binary logic combination of several triggers and specific conditions in terms of selectivity, the elimination of false positives or the reduction of undesired secondary effects. In the recent years some first examples for such approaches have been reported. Some are closer to the reality than others, but beyond any doubt all of them contributed to a consolidation of molecular logic in fields “outside the silicon box”.<sup>[68]</sup> Another focus of this Review is on intelligent materials. While at the moment the logically-motivated response of such materials is often read by monitoring conveniently observable properties like nanoparticle aggregation, some of them can be relatively straightforward imagined in relation to drug delivery. Others, often based on quantum dots, will be interesting for imaging with dependence on the combinational presence of certain specific parameters. The list of potential applications could be expanded even more, but it is not the objective of this Review to speculate or to create unrealistic expectations. The final benefits for real applications will be dependent on the imagination and skills of researchers in the multidisciplinary ambience of chemistry, physics, life sciences, and engineering. We hope that the examples compiled in this Review may stimulate new approaches and research efforts within the field of molecular information processing.

### **Acknowledgements**

The authors are indebted for the financial support by the Junta de Andalucía, Seville (grant FQM-3685 for U.P. and PhD fellowship for V.F.P.), the Swedish Research Council (grant 622-2010-280 for J.A.), the European Research Council (grant ERC FP7/2007–2013 No. 203952 for J.A.), and the U. S. National Science Foundation (grant CHE-0846943 for D.G.).

## References

- [1] A. P. de Silva, H. Q. N. Gunaratne, C. P. McCoy, *Nature* **1993**, *364*, 42-44.
- [2] J. Andréasson, U. Pischel, *Chem. Soc. Rev.* **2010**, *39*, 174-188.
- [3] V. Balzani, A. Credi, M. Venturi, *ChemPhysChem* **2003**, *4*, 49-59.
- [4] A. P. de Silva, *Chem. Asian J.* **2011**, *6*, 750-766.
- [5] A. P. de Silva, S. Uchiyama, *Nat. Nanotechnol.* **2007**, *2*, 399-410.
- [6] D. Gust, J. Andréasson, U. Pischel, T. A. Moore, A. L. Moore, *Chem. Commun.* **2012**, *48*, 1947-1957.
- [7] D. Gust, T. A. Moore, A. L. Moore, *Chem. Commun.* **2006**, 1169-1178.
- [8] E. Katz, V. Privman, *Chem. Soc. Rev.* **2010**, *39*, 1835-1857.
- [9] U. Pischel, *Angew. Chem.* **2007**, *119*, 4100-4115; *Angew. Chem. Int. Ed.* **2007**, *46*, 4026-4040.
- [10] U. Pischel, *Angew. Chem.* **2010**, *122*, 1396-1398; *Angew. Chem. Int. Ed.* **2010**, *49*, 1356-1358.
- [11] K. Szaciłowski, *Chem. Rev.* **2008**, *108*, 3481-3548.
- [12] O. A. Bozdemir, R. Guliyev, O. Buyukcakir, S. Selcuk, S. Kolemen, G. Gulseren, T. Nalbantoglu, H. Boyaci, E. U. Akkaya, *J. Am. Chem. Soc.* **2010**, *132*, 8029-8036.
- [13] D. Margulies, G. Melman, A. Shanzer, *J. Am. Chem. Soc.* **2006**, *128*, 4865-4871.
- [14] M. Amelia, M. Baroncini, A. Credi, *Angew. Chem.* **2008**, *120*, 6336-6339; *Angew. Chem. Int. Ed.* **2008**, *47*, 6240-6243.
- [15] J. Andréasson, S. D. Straight, S. Bandyopadhyay, R. H. Mitchell, T. A. Moore, A. L. Moore, D. Gust, *J. Phys. Chem. C* **2007**, *111*, 14274-14278.

- [16] J. Andréasson, S. D. Straight, S. Bandyopadhyay, R. H. Mitchell, T. A. Moore, A. L. Moore, D. Gust, *Angew. Chem.* **2007**, *119*, 976-979; *Angew. Chem. Int. Ed.* **2007**, *46*, 958-961.
- [17] E. Pérez-Inestrosa, J. M. Montenegro, D. Collado, R. Suau, *Chem. Commun.* **2008**, 1085-1087.
- [18] J. Andréasson, S. D. Straight, T. A. Moore, A. L. Moore, D. Gust, *J. Am. Chem. Soc.* **2008**, *130*, 11122-11128.
- [19] P. Ceroni, G. Bergamini, V. Balzani, *Angew. Chem.* **2009**, *121*, 8668-8670; *Angew. Chem. Int. Ed.* **2009**, *48*, 8516-8518.
- [20] Z. Q. Guo, W. H. Zhu, L. J. Shen, H. Tian, *Angew. Chem.* **2007**, *119*, 5645-5649; *Angew. Chem. Int. Ed.* **2007**, *46*, 5549-5553.
- [21] J. Andréasson, S. D. Straight, T. A. Moore, A. L. Moore, D. Gust, *Chem. Eur. J.* **2009**, *15*, 3936-3939.
- [22] D. Margulies, C. E. Felder, G. Melman, A. Shanzer, *J. Am. Chem. Soc.* **2007**, *129*, 347-354.
- [23] P. Remón, M. Hammarson, S. M. Li, A. Kahnt, U. Pischel, J. Andréasson, *Chem. Eur. J.* **2011**, *17*, 6492-6500.
- [24] G. Strack, M. Ornatska, M. Pita, E. Katz, *J. Am. Chem. Soc.* **2008**, *130*, 4234-4235.
- [25] W. Sun, C. Zhou, C. H. Xu, C. J. Fang, C. Zhang, Z. X. Li, C. H. Yan, *Chem. Eur. J.* **2008**, *14*, 6342-6351.
- [26] M. Suresh, A. Ghosh, A. Das, *Chem. Commun.* **2008**, 3906-3908.
- [27] R. Baron, A. Onopriyenko, E. Katz, O. Lioubashevski, I. Willner, S. Wang, H. Tian, *Chem. Commun.* **2006**, 2147-2149.

- [28] G. de Ruiter, L. Motiei, J. Choudhury, N. Oded, M. E. van der Boom, *Angew. Chem.* **2010**, *122*, 4890-4893; *Angew. Chem. Int. Ed.* **2010**, *49*, 4780-4783.
- [29] G. de Ruiter, E. Tartakovsky, N. Oded, M. E. van der Boom, *Angew. Chem.* **2010**, *122*, 173-176; *Angew. Chem. Int. Ed.* **2010**, *49*, 169-172.
- [30] G. de Ruiter, M. E. van der Boom, *Acc. Chem. Res.* **2011**, *44*, 563-573.
- [31] G. de Ruiter, M. E. van der Boom, *J. Mater. Chem.* **2011**, *21*, 17575-17581.
- [32] V. F. Pais, P. Remón, D. Collado, J. Andréasson, E. Pérez-Inestrosa, U. Pischel, *Org. Lett.* **2011**, *13*, 5572-5575.
- [33] U. Pischel, J. Andréasson, *New J. Chem.* **2010**, *34*, 2701-2703.
- [34] P. Remón, M. Bälter, S. M. Li, J. Andréasson, U. Pischel, *J. Am. Chem. Soc.* **2011**, *133*, 20742-20745.
- [35] G. Dilek, E. U. Akkaya, *Tetrahedron Lett.* **2000**, *41*, 3721-3724.
- [36] R. Ferreira, P. Remón, U. Pischel, *J. Phys. Chem. C* **2009**, *113*, 5805-5811.
- [37] R. Guliyev, S. Ozturk, Z. Kostereli, E. U. Akkaya, *Angew. Chem.* **2011**, *123*, 10000-10005; *Angew. Chem. Int. Ed.* **2011**, *50*, 9826-9831.
- [38] B. M. Frezza, S. L. Cockroft, M. R. Ghadiri, *J. Am. Chem. Soc.* **2007**, *129*, 14875-14879.
- [39] T. Gupta, M. E. van der Boom, *Angew. Chem.* **2008**, *120*, 5402-5406; *Angew. Chem. Int. Ed.* **2008**, *47*, 5322-5326.
- [40] T. Niazov, R. Baron, E. Katz, O. Lioubashevski, I. Willner, *Proc. Natl. Acad. Sci. U. S. A.* **2006**, *103*, 17160-17163.
- [41] F. M. Raymo, S. Giordani, *Org. Lett.* **2001**, *3*, 3475-3478.
- [42] F. M. Raymo, S. Giordani, *Org. Lett.* **2001**, *3*, 1833-1836.
- [43] F. Remacle, S. Speiser, R. D. Levine, *J. Phys. Chem. B* **2001**, *105*, 5589-5591.

- [44] G. Seelig, D. Soloveichik, D. Y. Zhang, E. Winfree, *Science* **2006**, *314*, 1585-1588.
- [45] S. Silvi, E. C. Constable, C. E. Housecroft, J. E. Beves, E. L. Dunphy, M. Tomasulo, F. M. Raymo, A. Credi, *Chem. Eur. J.* **2009**, *15*, 178-185.
- [46] K. Szaciłowski, *Chem. Eur. J.* **2004**, *10*, 2520-2528.
- [47] A. P. de Silva, N. D. McClenaghan, *Chem. Eur. J.* **2002**, *8*, 4935-4945.
- [48] A. P. de Silva, N. D. McClenaghan, *J. Am. Chem. Soc.* **2000**, *122*, 3965-3966.
- [49] X. F. Guo, D. Q. Zhang, G. X. Zhang, D. B. Zhu, *J. Phys. Chem. B* **2004**, *108*, 11942-11945.
- [50] S. J. Langford, T. Yann, *J. Am. Chem. Soc.* **2003**, *125*, 14951.
- [51] S. J. Langford, T. Yann, *J. Am. Chem. Soc.* **2003**, *125*, 11198-11199.
- [52] D. Margulies, G. Melman, A. Shanzer, *Nat. Mater.* **2005**, *4*, 768-771.
- [53] J. Andréasson, U. Pischel, S. D. Straight, T. A. Moore, A. L. Moore, D. Gust, *J. Am. Chem. Soc.* **2011**, *133*, 11641-11648.
- [54] F. M. Raymo, M. Tomasulo, *J. Phys. Chem. A* **2005**, *109*, 7343-7352.
- [55] Because both FG photochromes are in the same isomeric form after each photonic input application, only four out of six theoretically possible constitutional isomers are relevant in this discussion.
- [56] D.-H. Qu, Q.-C. Wang, H. Tian, *Angew. Chem.* **2005**, *117*, 5430-5433; *Angew. Chem. Int. Ed.* **2005**, *44*, 5296-5299.
- [57] J. Andréasson, G. Kodis, Y. Terazono, P. A. Liddell, S. Bandyopadhyay, R. H. Mitchell, T. A. Moore, A. L. Moore, D. Gust, *J. Am. Chem. Soc.* **2004**, *126*, 15926-15927.

- [58] J. Andréasson, S. D. Straight, G. Kodis, C. D. Park, M. Hambourger, M. Gervaldo, B. Albinsson, T. A. Moore, A. L. Moore, D. Gust, *J. Am. Chem. Soc.* **2006**, *128*, 16259-16265.
- [59] P. Remón, R. Ferreira, J.-M. Montenegro, R. Suau, E. Pérez-Inestrosa, U. Pischel, *ChemPhysChem* **2009**, *10*, 2004-2007.
- [60] M. Semeraro, A. Credi, *J. Phys. Chem. C* **2010**, *114*, 3209-3214.
- [61] D. C. Magri, G. J. Brown, G. D. McClean, A. P. de Silva, *J. Am. Chem. Soc.* **2006**, *128*, 4950-4951.
- [62] D. Margulies, A. D. Hamilton, *J. Am. Chem. Soc.* **2009**, *131*, 9142-9143.
- [63] T. Konry, D. R. Walt, *J. Am. Chem. Soc.* **2009**, *131*, 13232-13233.
- [64] J. Halánek, J. R. Windmiller, J. Zhou, M. C. Chuang, P. Santhosh, G. Strack, M. A. Arugula, S. Chinnapareddy, V. Bocharova, J. Wang, E. Katz, *Analyst* **2010**, *135*, 2249-2259.
- [65] M. Privman, T. K. Tam, V. Bocharova, J. Halánek, J. Wang, E. Katz, *ACS Appl. Mater. Interfaces* **2011**, *3*, 1620-1623.
- [66] Y. Benenson, B. Gil, U. Ben-Dor, R. Adar, E. Shapiro, *Nature* **2004**, *429*, 423-429.
- [67] Z. Xie, L. Wroblewska, L. Prochazka, R. Weiss, Y. Benenson, *Science* **2011**, *333*, 1307-1311.
- [68] S. Ozlem, E. U. Akkaya, *J. Am. Chem. Soc.* **2009**, *131*, 48-49.
- [69] R. J. Amir, M. Popkov, R. A. Lerner, C. F. Barbas III, D. Shabat, *Angew. Chem.* **2005**, *117*, 4452-4455; *Angew. Chem. Int. Ed.* **2005**, *44*, 4378-4381.
- [70] M. Hammarson, J. Andersson, S. M. Li, P. Lincoln, J. Andréasson, *Chem. Commun.* **2010**, *46*, 7130-7132.

- [71] J. R. Nilsson, S. M. Li, B. Önfelt, J. Andréasson, *Chem. Commun.* **2011**, *47*, 11020-11022.
- [72] S. Muramatsu, K. Kinbara, H. Taguchi, N. Ishii, T. Aida, *J. Am. Chem. Soc.* **2006**, *128*, 3764-3769.
- [73] C. Parente Carvalho, V. D. Uzunova, J. P. Da Silva, W. M. Nau, U. Pischel, *Chem. Commun.* **2011**, *47*, 8793-8795.
- [74] U. Pischel, V. D. Uzunova, P. Remón, W. M. Nau, *Chem. Commun.* **2010**, *46*, 2635-2637.
- [75] S. Angelos, Y. W. Yang, N. M. Khashab, J. F. Stoddart, J. I. Zink, *J. Am. Chem. Soc.* **2009**, *131*, 11344-11346.
- [76] M. W. Ambrogio, C. R. Thomas, Y. L. Zhao, J. I. Zink, J. F. Stoddart, *Acc. Chem. Res.* **2011**, *44*, 903-913.
- [77] D. Ishii, K. Kinbara, Y. Ishida, N. Ishii, M. Okochi, M. Yohda, T. Aida, *Nature* **2003**, *423*, 628-632.
- [78] J. W. Liu, Y. Lu, *Adv. Mater.* **2006**, *18*, 1667-1671.
- [79] B.-C. Yin, B.-C. Ye, H. Wang, Z. Zhu, W. Tan, *Chem. Commun.* **2012**, *48*, 1248-1250.
- [80] S. Bi, Y. M. Yan, S. Y. Hao, S. S. Zhang, *Angew. Chem.* **2010**, *122*, 4540-4544; *Angew. Chem. Int. Ed.* **2010**, *49*, 4438-4442.
- [81] G. von Maltzahn, T. J. Harris, J. H. Park, D. H. Min, A. J. Schmidt, M. J. Sailor, S. N. Bhatia, *J. Am. Chem. Soc.* **2007**, *129*, 6064-6065.
- [82] M. Pita, M. Krämer, J. Zhou, A. Poghossian, M. J. Schöning, V. M. Fernandez, E. Katz, *ACS Nano* **2008**, *2*, 2160-2166.
- [83] M. Motornov, J. Zhou, M. Pita, V. Gopishetty, I. Tokarev, E. Katz, S. Minko, *Nano Lett.* **2008**, *8*, 2993-2997.

- [84] H. J. Schneider, R. M. Strongin, *Acc. Chem. Res.* **2009**, *42*, 1489-1500.
- [85] H. J. Schneider, L. Tianjun, N. Lomadze, B. Palm, *Adv. Mater.* **2004**, *16*, 613-615.
- [86] N. Lomadze, H. J. Schneider, *Tetrahedron Lett.* **2005**, *46*, 751-754.
- [87] K. Kato, H. J. Schneider, *Langmuir* **2007**, *23*, 10741-10745.
- [88] I. Tokarev, V. Gopishetty, J. Zhou, M. Pita, M. Motornov, E. Katz, S. Minko, *ACS Appl. Mater. Interfaces* **2009**, *1*, 532-536.
- [89] A. P. de Silva, M. R. James, B. O. F. McKinney, D. A. Pears, S. M. Weir, *Nat. Mater.* **2006**, *5*, 787-790.
- [90] A. W. Czarnik, *Curr. Opin. Chem. Biol.* **1997**, *1*, 60-66.
- [91] L. X. Mu, W. S. Shi, G. W. She, J. C. Chang, S. T. Lee, *Angew. Chem.* **2009**, *121*, 3521-3524; *Angew. Chem. Int. Ed.* **2009**, *48*, 3469-3472.
- [92] X. Tian, Z. P. Dong, Y. F. Huang, J. T. Ma, *Colloids Surf., A* **2011**, *387*, 29-34.
- [93] S. Giordani, F. M. Raymo, *Org. Lett.* **2003**, *5*, 3559-3562.
- [94] J. Matsui, T. Sodeyama, K. Tamaki, N. Sugimoto, *Chem. Commun.* **2006**, 3217-3219.
- [95] C. P. Collier, E. W. Wong, M. Belohradský, F. M. Raymo, J. F. Stoddart, P. J. Kuekes, R. S. Williams, J. R. Heath, *Science* **1999**, *285*, 391-394.
- [96] C. P. Collier, G. Mattersteig, E. W. Wong, Y. Luo, K. Beverly, J. Sampaio, F. M. Raymo, J. F. Stoddart, J. R. Heath, *Science* **2000**, *289*, 1172-1175.
- [97] J. E. Green, J. W. Choi, A. Boukai, Y. Bunimovich, E. Johnston-Halperin, E. DeIonno, Y. Luo, B. A. Sheriff, K. Xu, Y. S. Shin, H.-R. Tseng, J. F. Stoddart, J. R. Heath, *Nature* **2007**, *445*, 414-417.
- [98] J. Matsui, M. Mitsuishi, A. Aoki, T. Miyashita, *Angew. Chem.* **2003**, *115*, 2374-2377; *Angew. Chem. Int. Ed.* **2003**, *42*, 2272-2275.

- [99] J. Matsui, M. Mitsuishi, A. Aoki, T. Miyashita, *J. Am. Chem. Soc.* **2004**, *126*, 3708-3709.
- [100] K. Szaciłowski, W. Macyk, G. Stochel, *J. Am. Chem. Soc.* **2006**, *128*, 4550-4551.
- [101] W. Macyk, G. Stochel, K. Szaciłowski, *Chem. Eur. J.* **2007**, *13*, 5676-5687.
- [102] N. Kaur, N. Singh, B. McCaughan, J. F. Callan, *Sens. Actuators, B* **2010**, *144*, 88-91.
- [103] R. Freeman, T. FINDER, I. Willner, *Angew. Chem.* **2009**, *121*, 7958-7961; *Angew. Chem. Int. Ed.* **2009**, *48*, 7818-7821.
- [104] S. Wang, W. Shen, Y. L. Feng, H. Tian, *Chem. Commun.* **2006**, 1497-1499.
- [105] J. W. Chung, S. J. Yoon, S. J. Lim, B. K. An, S. Y. Park, *Angew. Chem.* **2009**, *121*, 7164-7168; *Angew. Chem. Int. Ed.* **2009**, *48*, 7030-7034.
- [106] S. Uchiyama, N. Kawai, A. P. de Silva, K. Iwai, *J. Am. Chem. Soc.* **2004**, *126*, 3032-3033.

## Legends of Schemes

**Scheme 1.** Structures of compounds which are not discussed in a separate scheme in this Review.

**Scheme 2.** Representation of the electronic circuit of a 4-2 encoder.

**Scheme 3.** Structures of the different states and input conditions which are involved in the logic switching of spiropyran **3**.

**Scheme 4.** a) Structure of the photochromic triad **7**. b) Photoisomerizations of the model chromophores corresponding to triad **7**.

**Scheme 5.** Photochromic interconversions in triad **7**. Both fulgimide photochromes are coded by the same abbreviation (FG).

**Scheme 6.** Sequential switching of triad **7** with 366 nm light and red light for the realization of a molecular keypad lock. Only one sequence yields the fluorescent FGc-DTEo isomer, corresponding to the open lock.

**Scheme 7.** Schematic representation of labelled microspheres for the recognition of bacterial DNA and IL-8 cytokine following AND and INH logic (see text).

**Scheme 8.** Enzymatic cascade for the identification of lesions which are characterized by high levels of lactate dehydrogenase (LDH) and alanine transaminase (ALT).

**Scheme 9.** a) Logic circuit representation for the diagnosis of prostate cancer based on the analysis of the over- or underexpression of specific mRNA markers. The output is constituted by the release of a drug. b) Working principle of the corresponding molecular automaton.

**Scheme 10.** Logic circuit representation corresponding to the analysis of microRNA over- or underexpression typical for HeLa cells. The output consists in the release of hBax protein and subsequent apoptosis of the tumor cell.

**Scheme 11.** Photosensitized singlet oxygen generation by the BODIPY derivative **9** which is activated by  $H^+$  and  $Na^+$  inputs according to AND logic.

**Scheme 12.** Doxorubicin release from pro-drug **10** triggered by enzymatic action of penicillin G amidase (PGA) or catalytic antibody (Ab) 38C2.

**Scheme 13.** Photo- and acidochromic switching of spiropyran **11**.

**Scheme 14.** Switching of the conformation of the azobenzene-modified chaperone GroEL by using ATP as chemical input and UV light irradiation as photonic input. Only in presence of both inputs the cargo (not shown, see text for details) can be released most efficiently (AND logic).

**Scheme 15.** Schematic representation of the opening of a nanovalve following AND logic with light and base as inputs.

**Scheme 16.** AND and OR logic based on the protease-triggered supramolecular assembly of  $Fe_3O_4$  nanoparticles.

**Scheme 17.** pH-induced switching of the ionization state of nanoparticle capping ligands coupled to an enzymatic cascade (pH decrease) or urease (pH increase for re-setting).

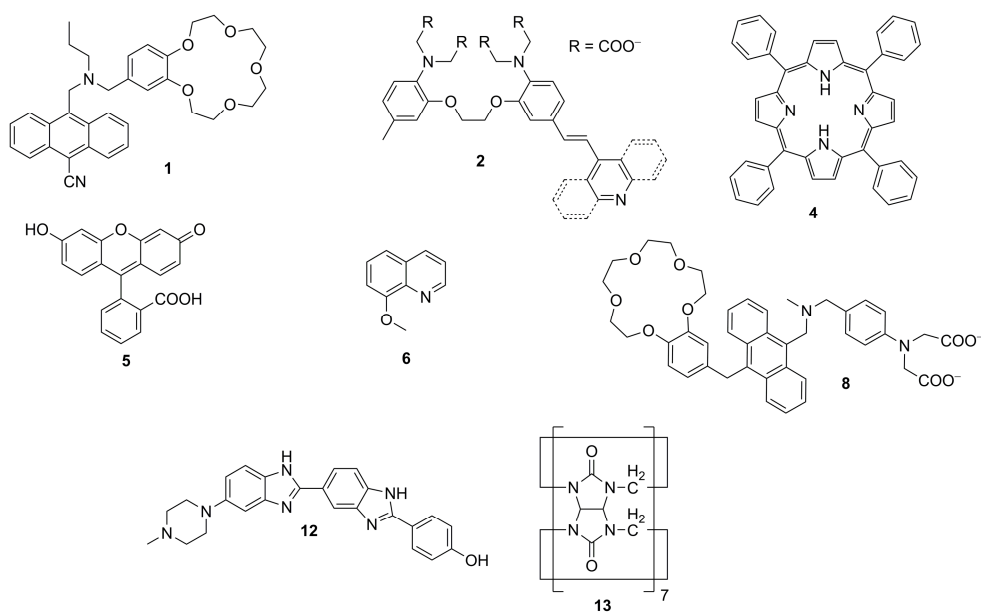
**Scheme 18.** Structures of a) an ethylenediamine-containing polymer and b) a polyethylenimine. Both were demonstrated as chemomechanical logic gates.

**Scheme 19.** Emission switching of luminescent quantum dots by recognition of ligand-specific inputs. a) *Off-on* emission switching by binding of  $H^+$  and  $Na^+$ . b) *On-off* emission switching by binding of  $Hg^{2+}$  or  $Ag^+$  to T- or C-rich oligonucleotides, respectively.

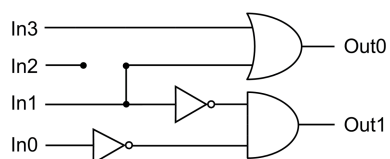
**Scheme 20.** Constituents of temperature-sensitive organogels with light-switchable dithienylethene photochromes.

**Scheme 21.** Temperature- and pH-controlled fluorescence switching of co-polymer **17** with integrated AND logic.

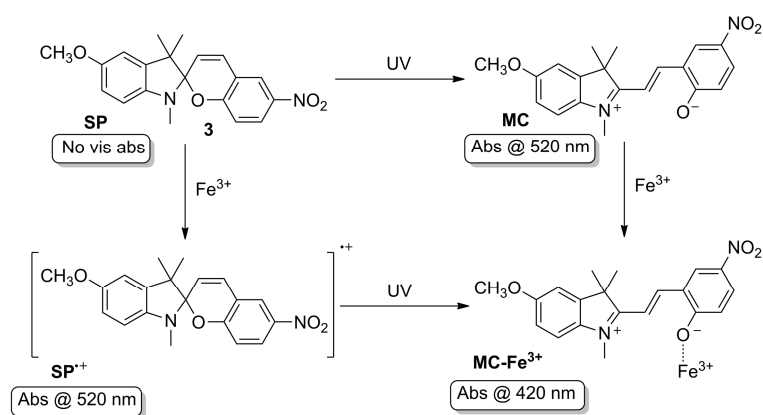
## Schemes



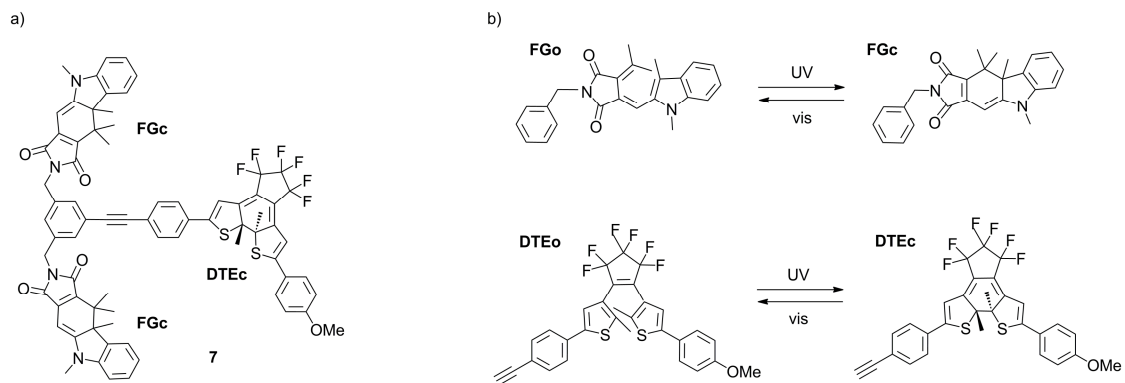
## Scheme 1



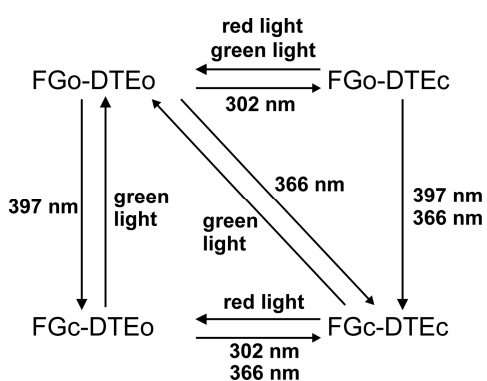
## Scheme 2



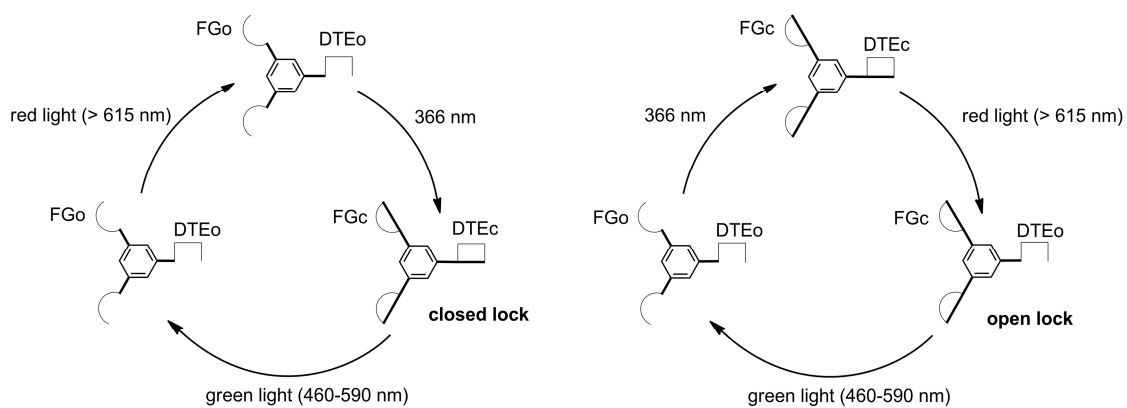
## Scheme 3



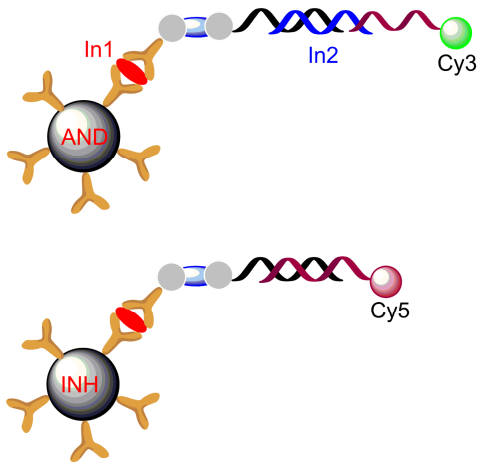
Scheme 4



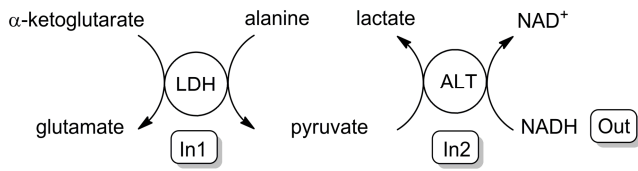
Scheme 5



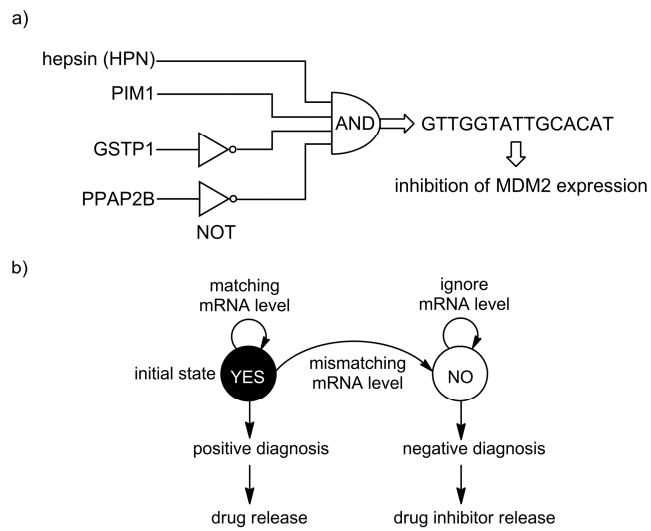
Scheme 6



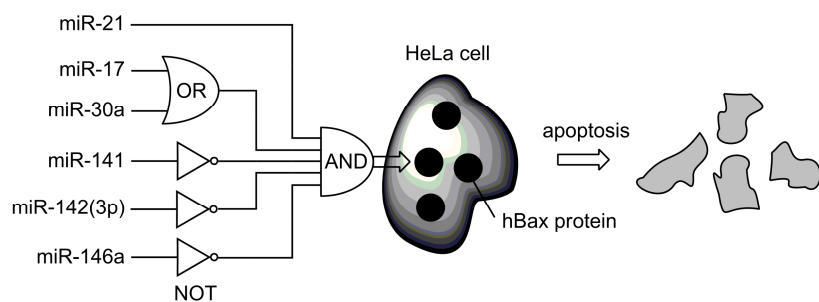
Scheme 7



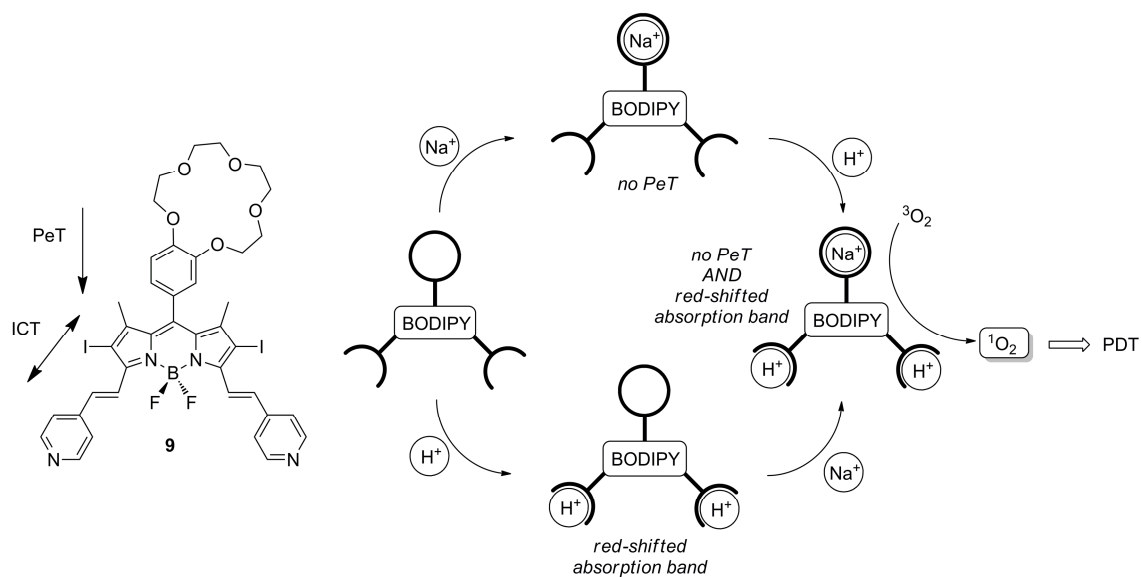
Scheme 8



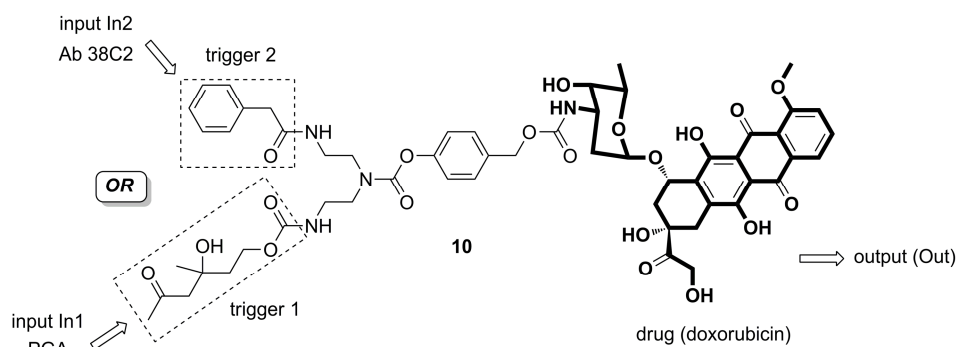
Scheme 9



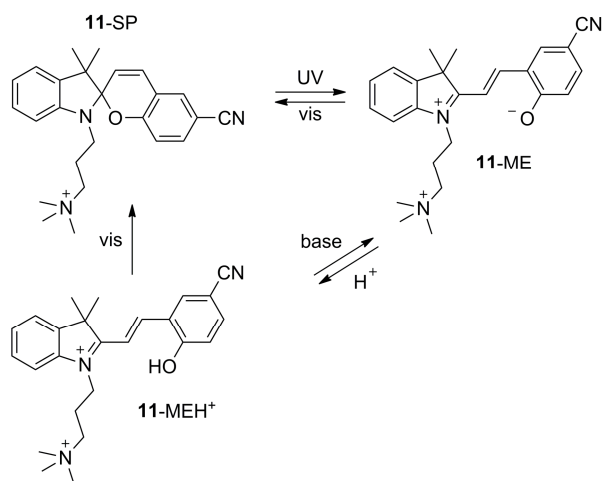
Scheme 10



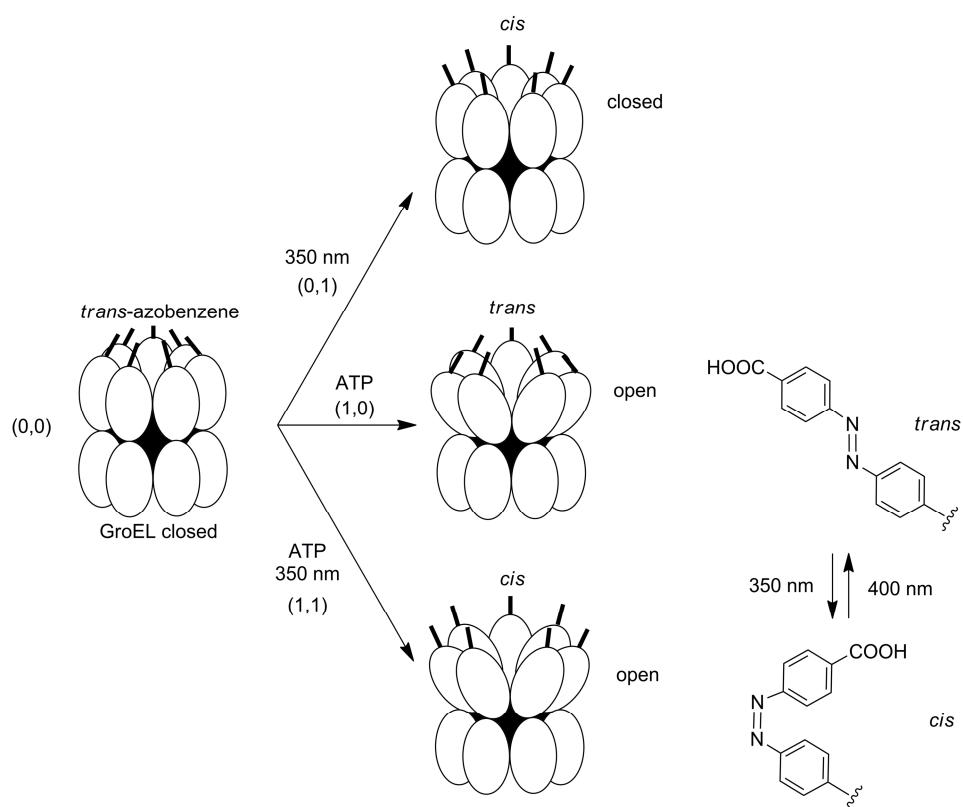
Scheme 11



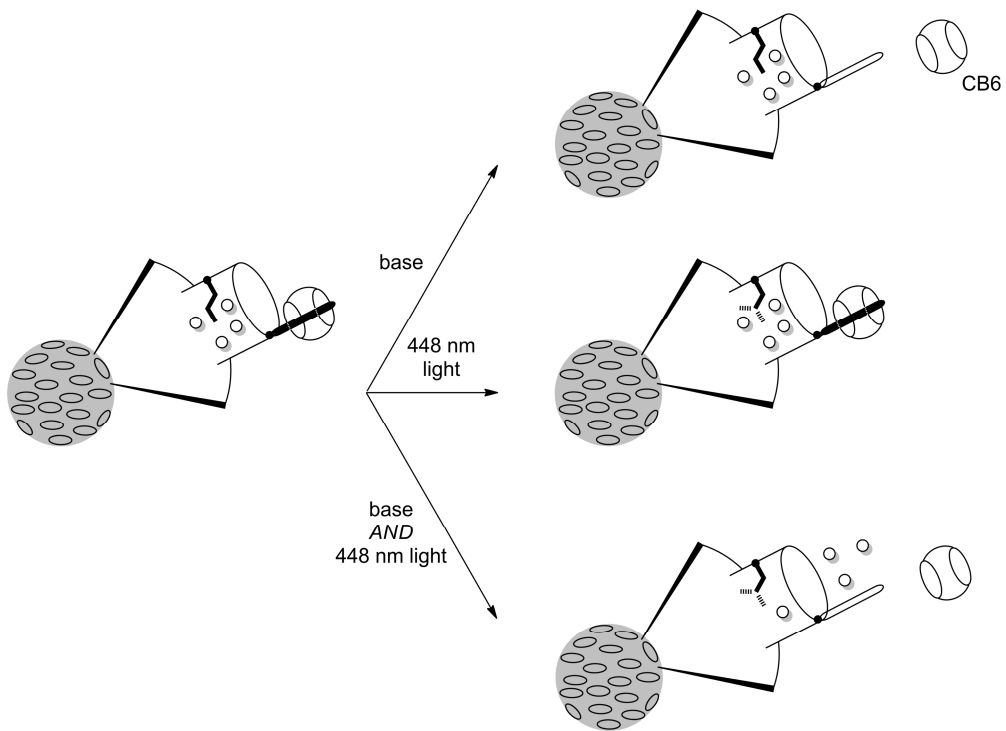
Scheme 12



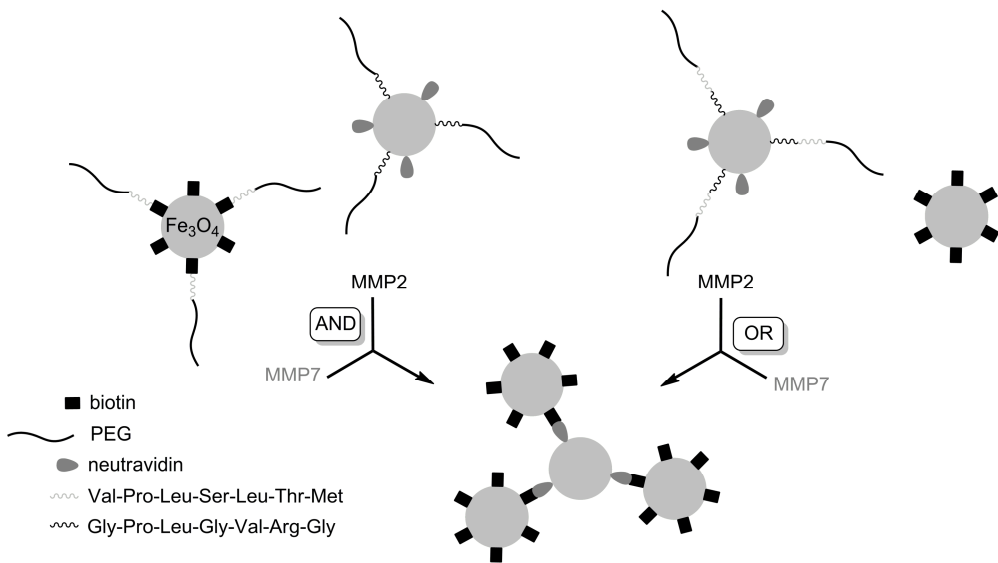
Scheme 13



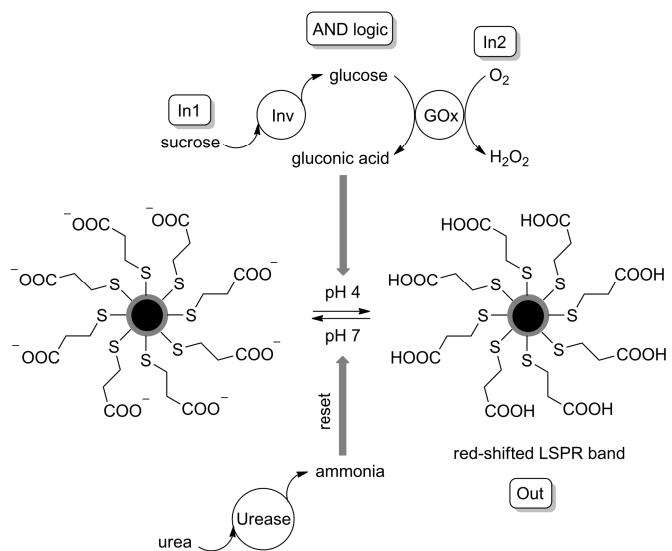
Scheme 14



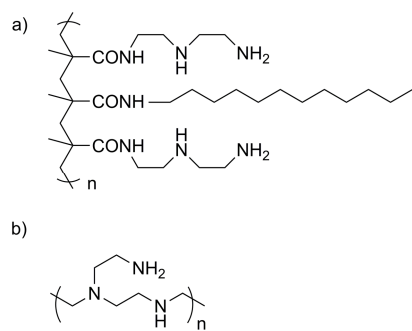
Scheme 15



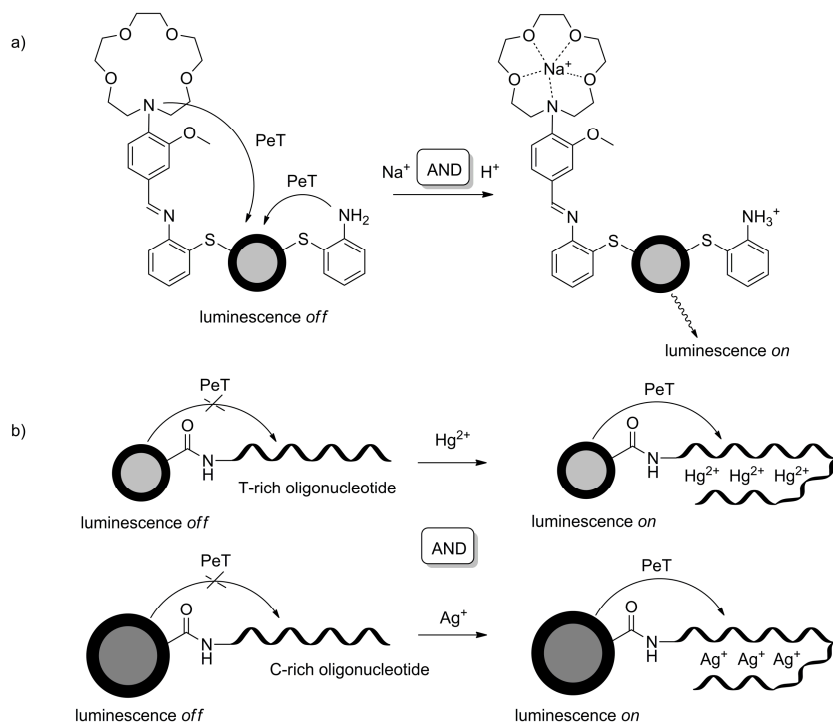
Scheme 16



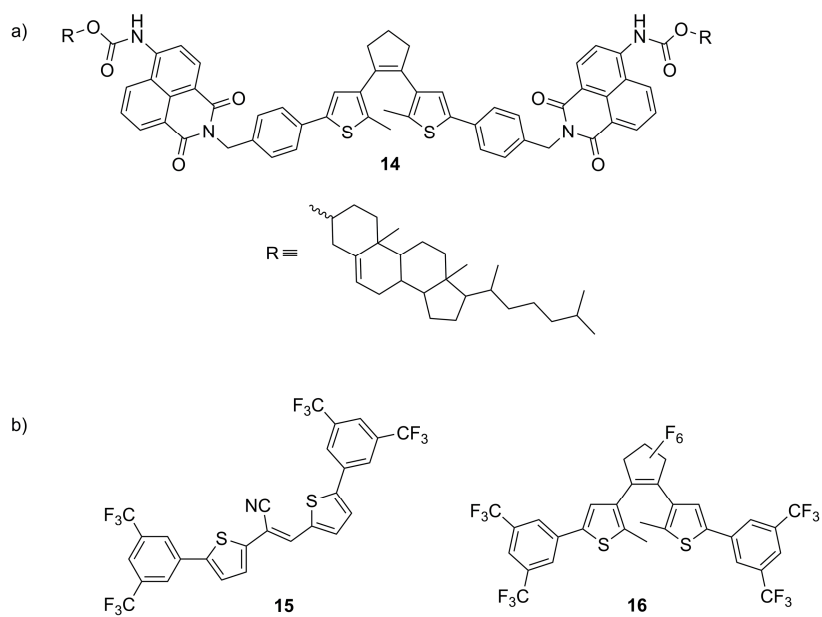
Scheme 17



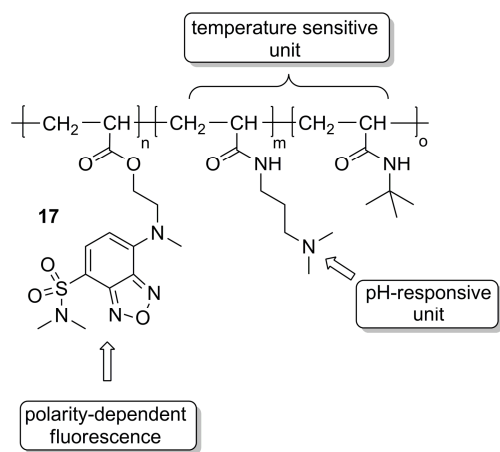
Scheme 18



Scheme 19



Scheme 20



Scheme 21

## Biographical Sketches and Author Portraits



**Uwe Pischel** is Lecturer in Organic Chemistry at the University of Huelva, Spain. His main research interests include supramolecular host-guest chemistry, fluorescent molecular switches, and molecular information processing.



**Joakim Andréasson** is Associate Professor in Physical Chemistry at Chalmers University of Technology, Sweden. He has research interests in photochromic molecules for molecular information processing and biological applications.



**Devens Gust** is Regents' Professor and Foundation Professor of Chemistry in the Department of Chemistry and Biochemistry at Arizona State University, Tempe, AZ, U. S. A. He serves as Director of the Center for Bio-Inspired Solar Fuel Production, a U. S. Department of Energy Supported Energy Frontier Research Center. He has research interests in organic photochemistry, molecular logic, and artificial photosynthesis.



**Vânia F. Pais** obtained a degree in Chemistry from the University of Évora (Portugal) in 2007 and is currently pursuing her PhD studies in the group of Dr. Pischel at the University of Huelva. Her research interests include molecular logic and switches and the study of novel fluorophore systems.

## Table of Contents Graph

**On its way:** In this Review the latest trends of the application of Boolean logic for molecular information processing are discussed. This includes the design of all-photonics devices, applications for pro-drug activation, drug delivery, diagnostics, and the creation of intelligent materials.

